CHEMICAL REVIEWS

Volume 95, Number 8 December 1995

The "Stealth" Liposome: A Prototypical Biomaterial

Danilo D. Lasic* and David Needham†

Liposome Technology Inc., Menlo Park, California, 94025, and Department of Mechanical Engineering and Materials Science, Duke University, Durham, North Carolina

Received December 2, 1992 (Revised Manuscript Received August 8, 1995)

Contents

* Corresponding address: D. D. Lasic, MegaBios Corp, 863-A Mitten Road, Burlingame, CA 94010.
† Duke University.

Introduction

In pharmacology the difference between effective and toxic concentration (the therapeutic window) of many potent drugs is very narrow and severely limits their utility. It has long been recognized that there is a tremendous need to be able to deliver drugs, especially highly toxic ones by targeting them to specific sites and avoiding, as much as possible, healthy organs, tissues, and cells. Many drug delivery systems can change the spatial and temporal distribution of the drug molecules (such as extend the availability of drug in blood circulation) and therefore improve the therapeutic index of the drug. However, none of the particulate drug carrier systems have so far shown substantial improvements in the pharmacokinetics and biodistribution of administered drug molecules, especially ones for cancer chemotherapy, and many infectious diseases and inflammations. With this need as a strong motivation, a new drug delivery system has emerged, the so called, Stealth liposome.[1]

In the Stealth liposome system, a drug is encapsulated in a specially designed, biocompatible, submicroscopic capsule that can evade the body's defenses, thus avoiding rapid uptake by the cells of reticuloendothelial system (RES) which are lo-

0009-2665/95/0795-2601$15.50/0

Danilo D. Lasic, Ph.D., is Senior Scientist at MegaBios, Burlingame, CA, where he is currently working with cationic liposomes in gene delivery. Previously, he was a senior scientist at Liposome Technology, Inc., where he led studies for theoretical understanding of long circulating liposomes as well as developed the first formulations for preclinical studies. In addition, he also actively participated in the scale up of the preparation of stealth liposomes laden with the anticancer agent, doxorubicin. Dr. Lasic graduated from the University of Ljubljana, Slovenia, in 1975 with a degree in physical chemistry. He received his M.Sci. in 1977 from the University of Ljubljana. He obtained his Ph.D. at the Institute J. Stefan, Solid State Physics Department in Ljubljana in 1979. After postdoctoral work with Dr. Charles Tanford at Duke and Dr. Helmut Hauser at ETH Zurich, he was a research fellow at the Institute J. Stefan in Ljubljana, and a visiting lecturer in the Department of Chemistry and a visiting scientist in the Department of Physics at the University of Waterloo in Canada. He then joined Liposome Technology, Inc., in Menlo Park, CA. Currently, he is studying cationic liposomes, DNA–liposome interactions, and DNA–lipid complexes for gene delivery and gene therapy. He has published more than 120 research papers as well as a monograph on liposomes (*Liposomes: from Physics to Applications*, Elsevier, 1993) and co-edited a book, *Stealth Liposomes* (CRC Press, 1995) and a series of four volumes on nonmedical applications of liposomes (*Theory and Basic Science, Models for Biological Phenomena, From Design to Microreactors*, and *From Gene Delivery to Diagnostics and Ecology*, CRC Press, 1995 and 1996, in press). His best known papers are the ones dealing with thermodynamics and the mechanism of vesicle formation, stability of liposomes, the origin of liposome stability in biological environments as well as the applications of drug-laden liposomes. He is a member of the editorial board of the *Journal of Liposome Research* and of *Current Opinion in Colloid and Interface Science*.

David Needham, Ph.D., is an Associate Professor in the Department of Mechanical Engineering and Materials Science, and the Center for Cellular and Biosurface Engineering at Duke University, Durham, NC. Professor Needham's research and teaching interests are focused on combining fundamental concepts in materials science, colloids, and interfaces in ordere to form a basis for characterizing: (1) the physical properties of biopolymers, microparticles, artificial membranes, biological membranes and cells; and (2) the interactions of these materials at interfaces of biological, technological, and medical importance. Using micropipet manipulation techniques and theoretical models, he examines basic physical features of composite cell membranes, capsules, coatings, and associated structures (that include the lipid bilayer), polymeric membrane surfaces, (including the natural cell surface or glycocalyx), and specific cell-adhesion receptors. Professor Needham graduated from Trent Polytechnic, Nottingham, England, in 1975 with a degree in Applied Chemistry. Following a period in industry with Manox (pigments) Ltd. in Manchester (1976–1977), he carried out graduate research with Professor Daniel D. Eley, F.R.S., at the University of Nottingham and received his Ph.D. in Physical Chemistry in 1980. After postdoctoral work with Professor Denis Haydon, F.R.S., in the Physiological Laboratory in Cambridge (1980–1983), and with Professor Evan Evans in the Department Academic Pathology in Vancouver Canada (1983–1987), he became Assistant Professor in the Department of Mechanical Engineering and Material Science at Duke University in 1987, and holds joint appointments in the Department Biomedical Engineering and the Duke Comprehensive Cancer Center. His honors include: recipient, F. I. R. S. T. Award, National Institutes of Health (1988–1993); Alfred M. Hunt Faculty Scholarship, Duke University (1988–1993); NATO/SERC (England) Fellowship (1983–1985); Oppenheimer Research Fellowship, Cambridge University (1982–1983). He is a member of the Biophysical and Biomedical Engineering Societies. Professor Needham has secured continuous funding since 1988 as PI or Co-PI on grants from Federal (NIH, NSF), and local (North Carolina Biotechnology Center), agencies and has collaborative projects with several industrial companies. He has published 45 papers in refereed journals and 11 chapters/monographs dealing with the mechanochemistry of lipid vesicle membranes and cells.

cated predominantly in liver and spleen. Because of this avoidance Stealth liposomes are more available to deliver drugs and other agents to specific target sites in the body. The Stealth liposome and similar sized Stealth particles therefore have the potential to improve a range of medical treatment strategies, including those aimed at vascular and nonvascular sites. They have expanded the applicability that was always anticipated for (but not fully realized by) "conventional" liposomes and other microcarrier-type drug delivery systems. Researchers in this area are currently addressing a whole range of issues from theoretical descriptions of the material properties of the Stealth liposomes to the performance of drug-laden Stealth liposomes in clinical trials.

In this review, we will present the developments that have occurred in the last few years and will attempt to derive lessons that will help to direct future work based on an approach that considers composition ↔ structure ↔ property relations, then together determine the performance-in-service of the materials involved. We will start by connecting back to the rather voluminous literature concerning conventional liposomes (the reader is referred to the collected works in refs 2−8). This discussion will serve to introduce not only a description of the liposome as a chemical and physical entity, but will also allow us to put into perspective the importance of the recent developments that have led to the emergence of the Stealth system. We will review what is known about the likely mechanisms that the immune and other systems impose on foreign particles, such as liposomes, when they are introduced into the body. Through this discussion, we will bring some rationale to the current and future design requirements of all Stealth microcarrier systems and, in fact, also of some other biosurfaces that must interface with biofluids. We shall attempt to couple as much as is possible at the moment, the available

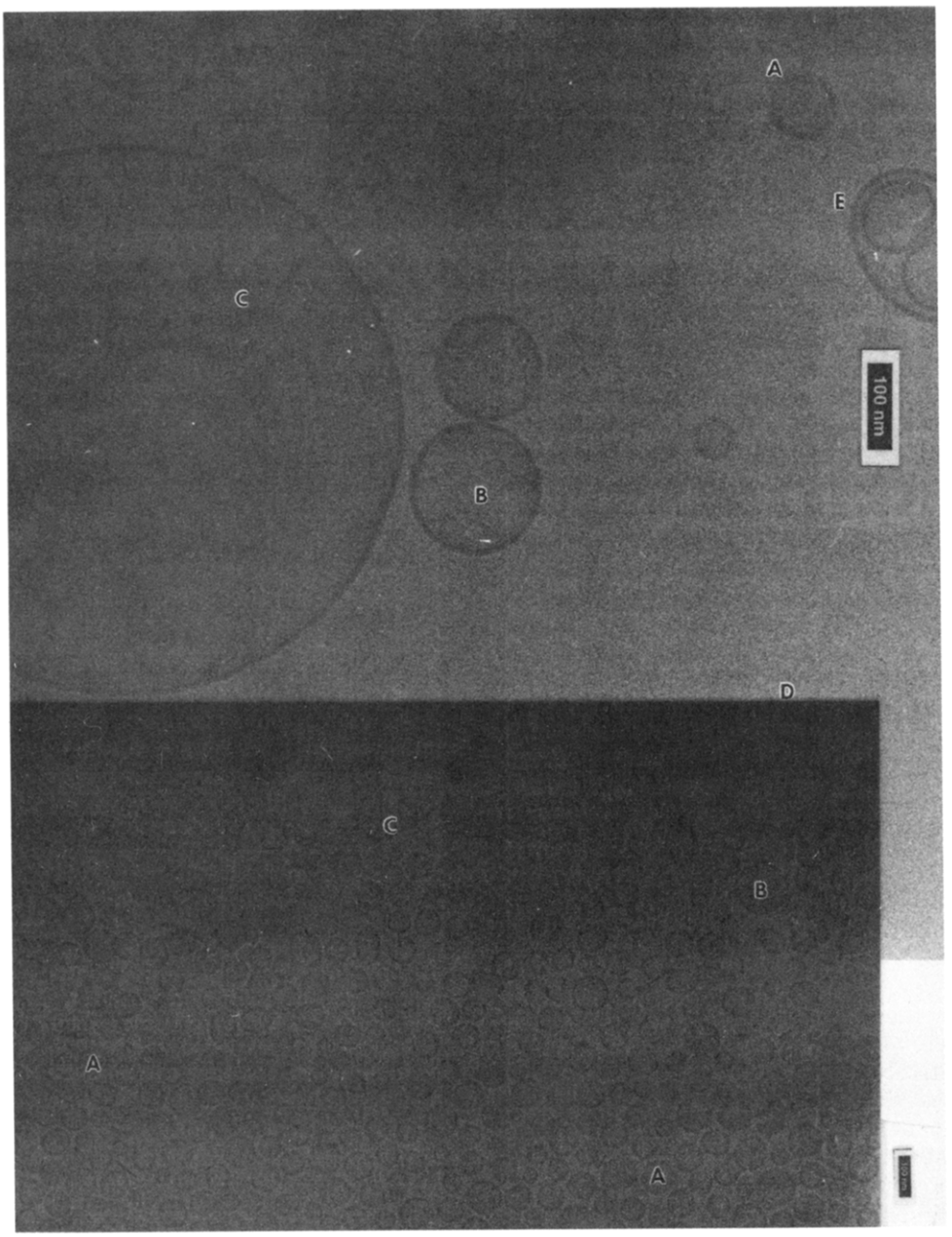

Figure 1. Cryoelectron micrograph of a heterogeneous liposome preparation. Small (a), large (b), and giant (c) unilamellar, and multilamellar vesicles (d), as well as multivesicular (e) liposome can be observed. Bars represent 100 nm. (Courtesy of P. Frederik, Limburg University, Maastricht.)

in vivo data with data that aim to quantitate the mechanical and interactive properties of liposomes in general, and the Stealth liposome in particular. We shall try to explain the complex in vivo behavior of liposomes on the basis of their colloidal, chemical, and mechanical properties which determine their in vivo reactivity, stability, and interaction characteristics.

1. Conventional Liposomes: A Brief Background into Their Composition, Structure, and Applications

Liposomes can be classified as association colloids, built up of amphiphatic lipid molecules that self-assemble in aqueous media into spherical, self-closed structures. Liposomes can be composed of either extracted and purified, naturally occurring lipids or (as used in model studies that require a pure preparation) many synthetic products that are commercially available. As shown in the cryoelectron micrograph in Figure 1 and the schematic diagram in Figure 2, the spherical liposome is an assembly of lipid molecules that are in a lamellar phase formed from two monolayers that are apposed back to back to give the bilayer membrane. Thus, liposomes are essentially spherical and can encapsulate aqueous media.[9] Liposome size can range over 3 orders of magnitude, from 10 of nanometers to 10 of micrometers, and they can contain one, several, or many (concentric) bilayer membranes. These structural differences are recognized by the respective designations small, large, and giant unilamellar vesicles (SUV, LUV, and GUV); oligolamellar vesicles (SOV, LOV, and GOV); and the most easily formed multilamellar vesicles (MLV).[3]

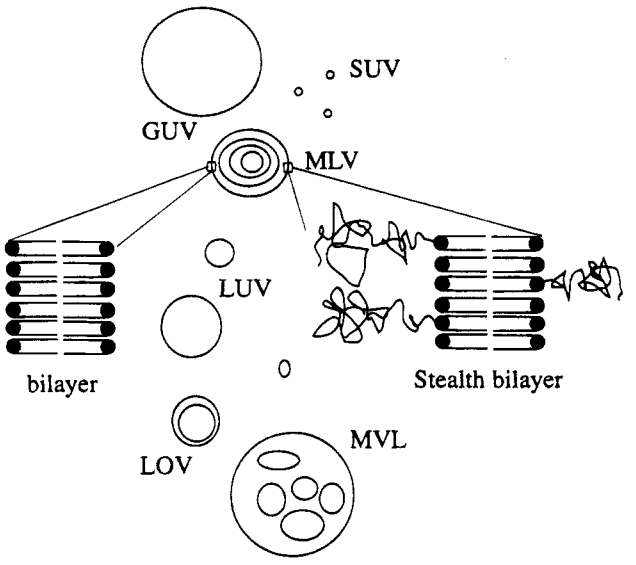

Figure 2. Schematic presentation of liposome bilayer and structure of liposomes. Normal bilayer is shown on left while polymer-grafted bilayer is shown on the right of multilamellar vesicles (MLV), multivesicular liposome (MVL), and giant, large, and small unilamellar vesicles (GUV, LUV, and SUV).

Every cell on the planet is surrounded by a membrane that has the same basic lipid bilayer structure as that exhibited by liposomes. Because of this, the lipid bilayer has been used extensively as a model system for studies that aim to decipher the complexities of cell membrane structure, properties, and function.[10] As with the cell, the lipid bilayer acts as a chemical, mechanical, and electrical barrier that sequesters an internal aqueous solution and separates it from the external milieu. Herein lies the basis for the technological utility of the liposome; it provides a relatively biocompatible system (biodegradable, absence of toxicity, and negligible induction of immune response) for the microencapsulation and sustained release of internally trapped aqueous soluble agents; and it can also act as an amphiphatic solvent with a wide spectrum of solubilizing power that can disperse otherwise immiscible components in aqueous media, such as the blood stream.

One of the most promising applications of liposomes has always been parenteral (administration elsewhere than the alimentary canal) drug delivery.[3-8] When compared to the fate of free drug, a variety of colloidal-sized drug carriers have been shown to change the biodistribution of entrapped or bound drug molecules in the body and to change the rate of uptake in specific organs and tissues.[3-8,10] This microparticle strategy has resulted in improved drug efficacy, reduced toxicity, or both. Liposomes became, for a variety of reasons, the most studied and used microparticle system. Apart from biocompatibility and naturally occurring constituents, from a research and manufacturing point of view, their size and surface properties can be well tailored during preparation.[10,11] Also, most of the limitations such as large-scale reproducible preparation, sterilization, and stability in storage and transit have been overcome.[10,12]

The majority of applications require intravenous administration, and so the "age-old" problem with liposomes, as with all foreign colloidal delivery systems, is that the particles are exposed to a range of nonspecific and specific sinks that act to deplete the injected dose from the blood stream. Although this uptake is long (minutes to a few hours) compared to the removal of free drug, it still severely compromises the usefulness of the circulating reservoir of encapsulated drug. Nevertheless, in several particular cases, conventional liposomes have provided a beneficial mode of action as drug delivery vehicles. In addition to the treatment of the diseases of phagocytic cells themselves some of the successful applications, which take advantage of the solubilizing and microencapsulation properties of liposomes, are shown in Table 1.

2. The Stealth Liposome: Definition, Developments, and Possible Mechanisms of Action

2.1. The "Stealth" Property

The body protects itself against pathogenic attack with a complex molecular and cellular defense system. Upon entering into the body, foreign substances get either excreted, digested, or passivated. In contrast to unmodified colloidal particles, which are recognized and, after opsonization (i.e., adsorption of proteins of immune system), taken up by macrophages, Stealth particles have specially engineered surface properties that enable them to evade this rapid uptake.[10] Arbitrarily, we define rapid uptake as being circulation half-times less than 2 h.

2.2. Developments

Several approaches have been developed that increase the circulation times of conventional lipo-

Table 1. Modes of Action of Liposomes in Pharmaceutical Formulations

liposome utility	example	disease states treated
solubilization	Amphotericin B, minoxidil	fungal infections
sustained-release	systematic antineoplastic drugs, hormones, corticosteroids	cancer, biotherapeutics
site-avoidance	Amphotericin B (kidneys), doxorubicin (heart)	fungal infection, cancer
drug protection	cytosine arabinoside, interleukins	cancer, etc.
passive targeting	immunomodulators, vaccines, antimalarials, macrophage-located diseases	cancer, MAI, tropical parasites
specific targeting	cells bearing specific antigens	wide therapeutic applicability
extravasation	leaky vasculature of tumors, inflammations, infections	cancer, infections
accumulation	prostaglandins	cardiovascular diseases
enhanced penetration	topical vehicles	dermatology
drug depot	lungs, subcutaneous, intramuscular, ocular	wide therapeutic applicability
intracellular delivery	DNA, genes, antisense oligonucleotides	gene therapy, bioengineering

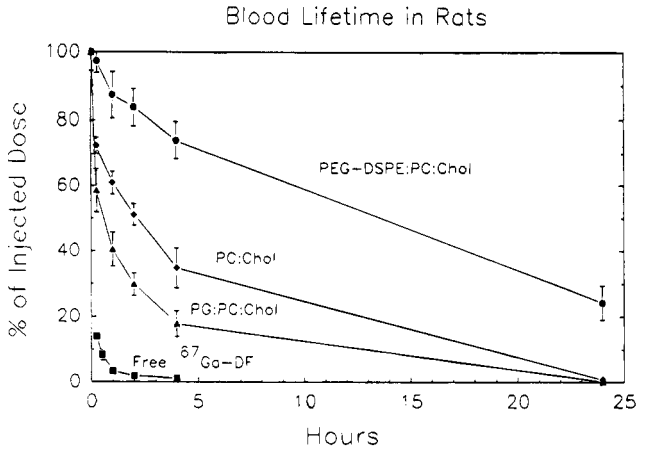

Figure 3. Blood clearance rates of different liposome preparations as measured by the radioactive tracers. For details see ref 20.

somes. For example, small, uncharged liposomes circulate longer while presaturation of RES with empty MLVs or suppression or elimination of immune system is medically questionable and certainly impractical.[10,13] Liposomes composed from phospholipids with saturated hydrocarbon chains, most notably stearic, and preferably containing high amounts of cholesterol, yielded the longest blood circulation times.[13] These improvements, coupled with the unavoidable stability problems of such uncharged formulations, however, were not significant enough to produce much advantage over existing nonliposomal treatments as can be judged from the fact that as of mid-1995 and after two decades of work there is only one parenteral liposomal product on the market, a SUV formulation of antifungal agent Amphotericin B, and even this one is only commercially available in some European countries. Subsequent approaches tried various surface modifications such as coatings with proteins[14] or glycolipids.[15] Later it was found that small and cholesterol-rich liposomes composed from lipids containing C18 saturated chains and doped with ganglioside G_{M1}[16] or hydrogenated plant phosphatidylinositol[17] at 5–10 mol % exhibited substantially improved blood circulation times.

The most important improvement was based on an analogy with efforts to improve circulation times of proteins by PEGylation[18] and nanoparticles with adsorbed block copolymers.[19] Liposomes with surface-grafted PEG chains were thus introduced[20–24] as reviewed in refs 25–28. Polymer-grafted liposomes showed from 1 up to 2 orders of magnitude longer circulation times and substantially altered the pharmacokinetics and biodistribution of encapsulated drug molecules.[29,30] Figure 3 shows the blood circulation times of various liposome preparations. [During the final revisions of this review we learned that FDA's Oncologic Drugs Advisory Committee voted unanimously (Washington, Feb 14, 1995) to recommend approval of doxorubicin in stealth liposomes, a product which is described below.]

2.3. PEGylated Phospholipid Molecules and the Preparation of Stealth Liposomes

Several ways to synthesize these molecules have been described in refs 25–27. The most common

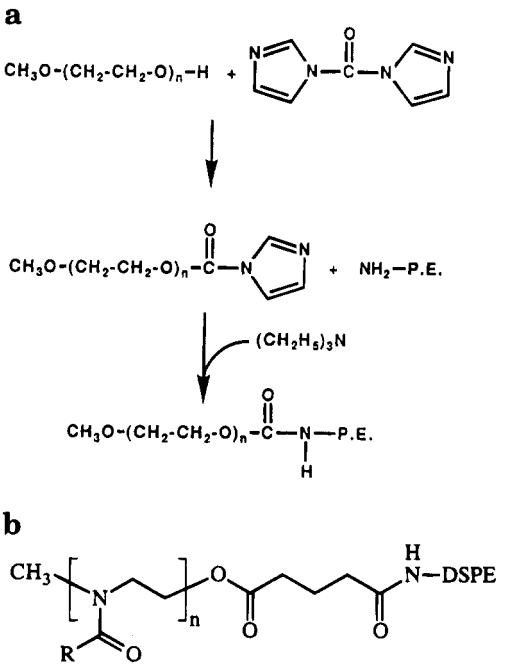

R = CH_3 for poly(2-methyl-2-oxazoline)
R = C_2H_5 for poly(2-ethyl-2-oxazoline)

Figure 4. (a) Chemical formula and chemical synthesis scheme for the methoxy polyoxyethylene carbamate derivative of phosphatidyl ethanolamine and (b) structural formula for poly(2-acyl-2-oxazoline).

reaction, which also produces a chemically very stable bond, is by coupling methoxy PEG, which has only one reactive end to the amino group on phosphatidylethanolamine via carbamate linkage using carbonyldiimidazole, as shown in Figure 4. For some purposes, however, one would prefer fast cleavage of polymer chains as can be achieved by different chemical linkages to further tailor pharmacokinetics and biodistribution of liposomes. Very recently, however, the search for targetable stealth liposomes has resulted in the synthesis of heterobifunctional PEG which enables coupling of antibodies to the far end of the grafted PEG chains.[31] Conjugation of conventional liposomes was normally achieved by incorporation of functionalized lipid component (maleimido- or carboxyphosphatidylethanolamine) which, after formation of vesicles, underwent an immunoglobulin conjugation process. The presence of PEG coating, however, interfered with the reaction itself, as well as the interaction of the immunoliposome with its target antigen. Heterobifunctional PEG can have several active groups at the far end, such as carboxylate or hydrazide, while the other end is attached to PE via amino-reactive succinimidyl carbonate group. Periodate-oxidized antibodies can bind to hydrazide groups.[32]

The polydispersity of the polymer varies according to the purity of the starting polymer and practically does not change after chemical linkage. Commercial grade material has a reported polydispersity index P, as defined by a ratio of weight over number average molecular weight, of 1.1, while BioTech grade has $P = 1.05$. A mass spectrum of commercial grade PEG 2000 is shown in Figure 5a, and the standard deviation of the symmetric distribution around 2000

a

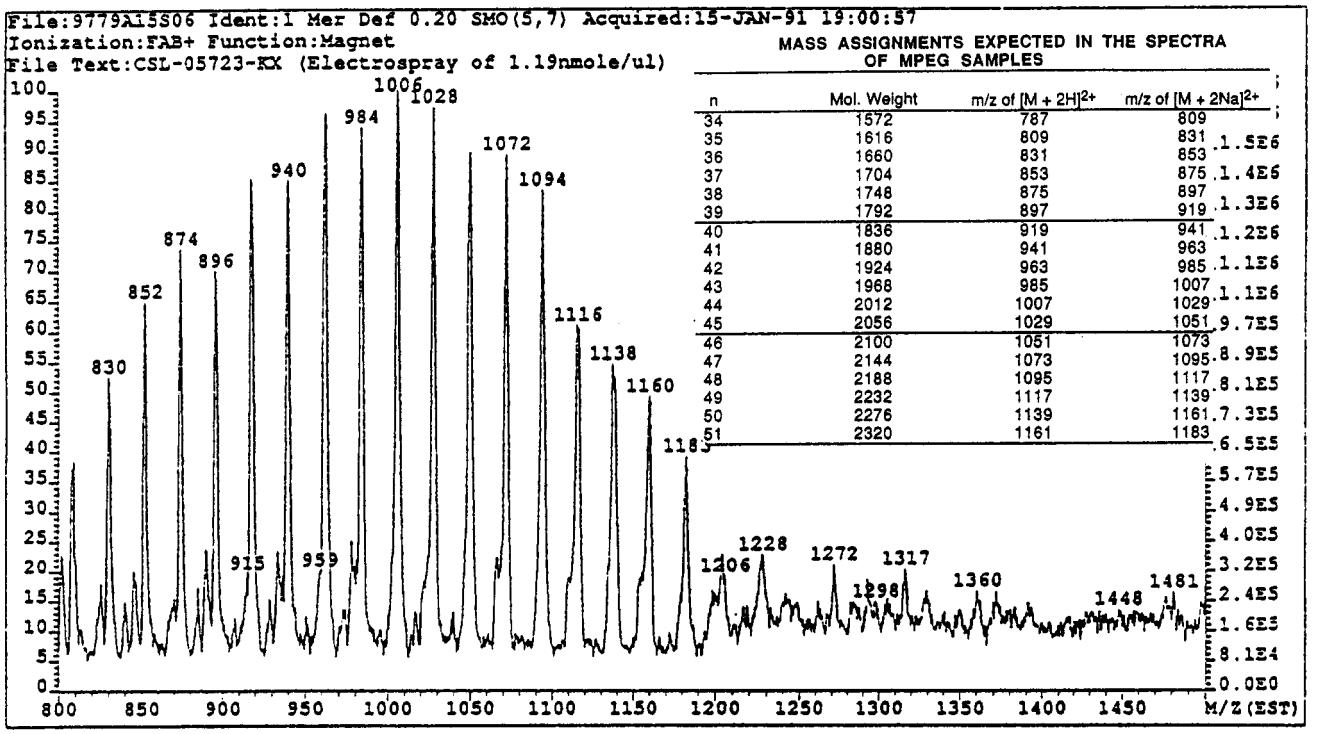

b

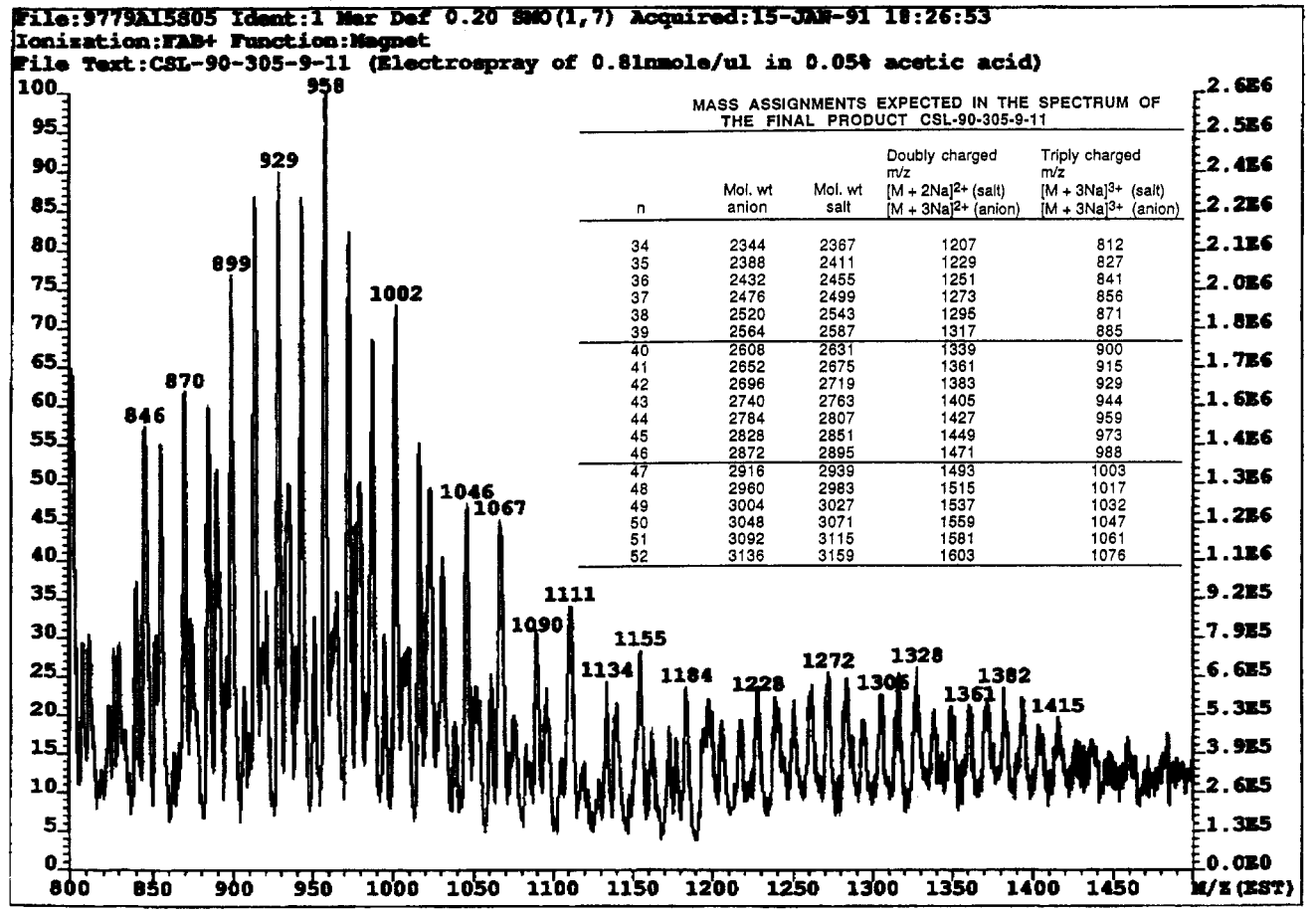

Figure 5. Mass spectra of metoxy PEG 2000 Da (a) and, after its coupling to DSPE, of ^{2000}PEG-DSPE (b). Spectra were recorded on VG Tribrid (EBEEQQ geometry) at sample flow rate 4 μL/mL (curtain gas 0.3L/min at 100 °C) and voltages at interface plate, nozzle, and needle were 3.17, 3.13, and 8.9 kV, respectively. At accelarating voltage 2.9 kV mass range m/z = 800 to m/z = 1500 were scanned (* s/scan, signal averaged for 20 min). Spectra as well as tabulated mass assignements, as expected from the spectra of both compounds, show that chemical reaction only shifts molecular weight for 772 Da. (Courtesy of J. Guthrie and S. Greenwald.)

Da is 400 Da, i.e. 67% of the polymer has degree a of polymerization 45 ± 9. Figure 5b shows that after linkage to the lipid, the polymer polydispersity does not change.

As used commercially, liposomes normally contain between 4 and 10 mol % of PEGylated lipid, in which the molecular weights of PEG is mostly 2000 and 5000 Da. At concentrations above 15−20 mol % the bilayers become unstable due to the increased lateral pressure among polymer chains.[32−34] Many different lipid compositions can be used, but because of the need to minimize lipid oxidation and leakage of the encapsulated molecules as well as cost, the most frequently used lipids are mixtures of hydrogenated soy lecithin, which consists predominantly of stearic chains,[10] and cholesterol. Liposomes can be produced by all the available liposome preparation methods with extrusion or microfluidization of thin film hydrated multilamellar dispersions being the most frequently used ones. Prolonged sonication may cleave polymer chains. The optimal size is between 70 and 200 nm; larger liposomes in general do not circulate as long while there are some indications that the same may hold true for smaller ones probably due to the leakage through fenestrations in blood vessels' walls. In any case, the carrying capacities of the smaller liposomes are too small and with a possible exception of very potent drugs and efficient loading techniques, they are not used. Obviously, drug molecules must be encapsulated in a stable manner so that long-circulating liposomes can deliver their cargo.

2.4. Other Stabilizing Polymers

All the reported long-circulating and polymer-coated liposomes contain PEG polymer. Anecdotal evidence exists that the use of poly-lactic acid and poly-glutamic acid did not result in any effective biological stabilization and that the use of block copolymers resulted in the vesicle leakage.

Although PEG has several special properties, such as high anisotropy of the monomer (i.e., is very thin polymer), and good solubility in polar and nonpolar solvents, there was no reason to expect it to be unique in rendering biological stability to liposomes. Indeed, recently two new polymers were described which conveyed long circulation times and low hepatospleenic uptake to liposomes. Poly(2-methyl-2-oxazolidine) (PMOZ) and poly(2-ethyl-2-oxazolidine) (PEOZ) with degree of polymerization ≈ 50 and linked via glutarate esters to DSPE, at 5 mol % in the bilayer, gave rise to very similar pharmacokinetics and biodistribution of liposomes as polyethylene glycol[35] (Figure 4b).

Amphiphilic polyacrylamide and poly(vinylpyrrolidone) containing liposomes also showed increased blood circulation although the prolongation was less significant. Because the general behavior of polymers should be similar, one can understand this effect by weaker hydrophobic anchoring as these two polymers were attached to dodecyl and palmitoyl chains.[36] Longer chains showed, as expected, longer circulation times. Relatively short BCT can be understood by the detergent depletion method for liposome preparation which may further decrease the fraction of these lipids which have higher aqueous solubility than other liposomal lipids.

In addition to those, there are undoubtedly many other polymers, including branched ones, which can render steric stability to liposomes.

2.5. Possible Mechanisms of Action

Liposome formulations containing PEGylated lipids have now prolonged encapsulated-drug circulation times to several days. Mechanisms of liposome blood clearance are, however, still not fully understood. It would seem that clearance must involve contact between liposomes and cells and molecules of the blood system. At least three underlying interfacial mechanisms, all of them based on improved liposomal colloidal stability, would appear to be involved:

2.5.1. Steric Stabilization of Liposomes (Colloidal)

Steric stabilization by the polymer opposes the mutual aggregation of unmodified liposomes (Figure 6) and would also appear to limit the interactions of liposomes with all other cellular surfaces in the blood system.[27] While polymers that are adsorbed or grafted onto a variety of substrates have been the subject of considerable theoretical and experimental study the first experimental measures of the mutual repulsive pressures that polymer-bearing lipid bilayer systems are expected to exert, were reported only recently (see section 4). With regard to liposomes there have been only few, rather qualitative, studies showing reduced aggregation and fusion[25,37−39] of PEG-bearing liposomes. Also, the binding capacity of immunoliposomes with attached antibodies was reduced in the presence of PEG-lipids.[27,39] Recent experiments have shown that PEG-coated liposomes are resistant to fusion in aqueous solutions up to the addition of 30 wt % of ^{2000}PEG free polymer while 25% of control vesicles exhibited mixing of aqueous contents.[40]

2.5.2. Evasion of RES (Biointerfacial)

Colloidal-sized particles are cleared from the blood circulation mostly by opsonization. In this process, various plasma components, especially immunoglobulins and complement factors, bind to foreign matter which consequently triggers their uptake by macrophages. Opsonization can also be nonimmunogenic, such as the adsorption of fibronectin. It is very likely that the presence of the bulky, nonionic, nonimmunogenic, hydrophilic (PEG) polymers on the liposome surface reduces the adsorption of opsonins. Studies on other PEG polymer-bearing surfaces have indicated that small molecular weight polymers (≤1000 g/mol) can inhibit protein adsorption,[41] and by inference, opsonizaton, but that larger molecular weights (18500 g/mol) are required to inhibit adhesion with cellular surfaces.[42−44]

2.5.3. Liposome Destruction by Nonimmune Components, e.g. Lipoproteins and Lipase Enzymes, etc. (Material/ Chemical Stability)

Polymer coating also significantly reduces interactions with other plasma components which can

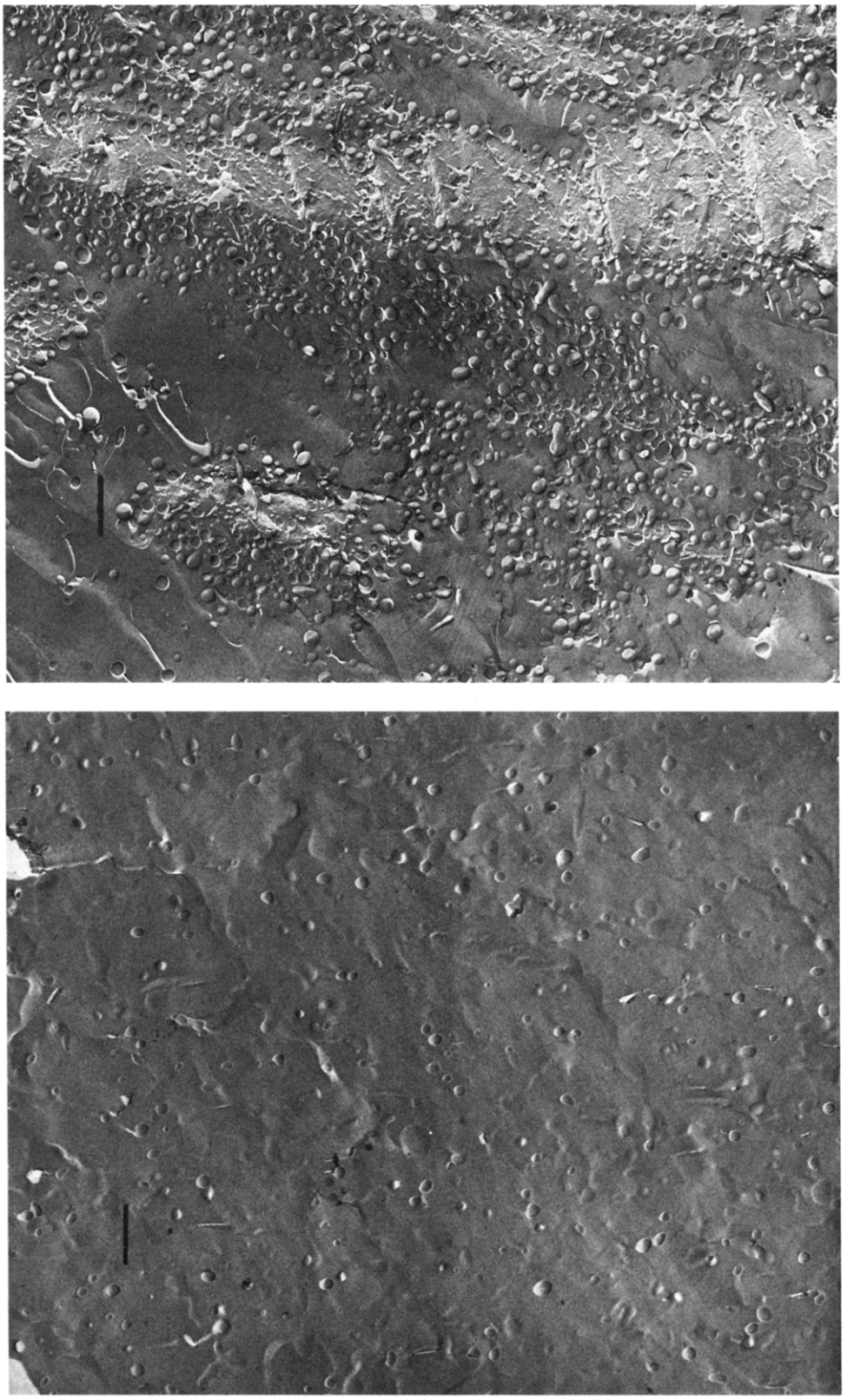

Figure 6. Freeze fracture electron micrographs of extruded conventional (egg phosphatidyl choline/cholesterol, 2/1, part a (top)) and stealth liposomes (part b (bottom)), same composition with exception that 4 mol % of EPC was substituted with ^{2000}PEG-DSPE). The aggregation of uncharged and not sterically stabilized liposomes could be clearly observed. Bars represent 500 nm. (Courtesy of J. Costello, UNC, Chapel Hill.)

destabilize liposomes upon contact or by exchange/depletion of lipids. This stability, of course, is also coupled to the mechanical characteristics of the bilayer itself. The higher mechanical stability of cholesterol-containing lipid bilayers has been shown to inhibit access of the bilayer's constituent lipids to attack by surface-active enzymes and to the dissolution of the lipids by lipoproteins.[12,45,46] Thus, although we do not expect that such small liposomes will be exposed to levels of surface stress that might

break the membranes, mechanical stability is an indicator of cohesion[47] and resistance to chemical attack. Reduced interaction with lipoproteins which deplete lipids from bilayers was shown in black lipid membranes containing 5 mol % ^{2000}PEG-DSPE as opposed to the ones with DSPE only.[48] The surface-grafted polymer must also exert some influence on chemical stability since it is likely that it inhibits access to the lipid surface for anything but the smallest molecules.[49] Thus the polymer barrier acts in concert with membrane cohesion in opposing physicochemical breakdown by enzymes, lipoproteins, and chylomicrons. Furthermore, in addition to improved colloidal stability, mechanical strength of the membranes is also important in order to more tightly bind PEG-lipid molecules in the bilayer.

3. Experimental and Results

Several experiments with liposomes have addressed aspects of the above mechanisms. The results from X-ray and surface force apparatus studies of the interbilayer interactions will be presented in section 4.2.7, after a brief introduction to the technique, mechanical properties of membranes, and interbilayer forces. We expect, that many more studies, from measuring protein interactions and adsorption using either vesicles, monolayers, or BLM, to the dynamics of the chains studied by spectroscopic techniques, will be performed.

3.1. Colloidal Stability

Only a few quantitative studies have been performed on the enhanced stability of sterically stabilized, i.e. polymer-bearing, liposomes. It was shown that the presence of surface-bound polymers increased stability of liposomes against exposure to plasma in vitro and Ca^{2+}-induced fusion, and decreased their aggregation in the presence of agglutinants.[37-39] In our hands, observations of giant vesicles as well as SUVs in optical and electron microscope (Figure 6), respectively, showed much weaker (or nonexistent) aggregation than in otherwise equivalent lecithin–cholesterol liposome systems. Furthermore, upon pelleting at 230000*g* for 24 h the solid pellet can be redispersed with no change of the size distribution while unmodified hydrogenated soy lecithin–cholesterol liposomes formed a compact (and much smaller) MLV pellet.[50] Small-angle neutron scattering and NMR experiments performed with these liposomes showed no changes in the spectra in fresh and half year old samples.[51,52] This is practically impossible to observe in conventional liposome samples.

3.2. Protein Adsorption

In the early 1980s it was realized that plasma proteins can react with liposomes in several different ways. Serum lipoproteins can destabilize the liposome membrane causing leakage of vesicle contents and potentially leading to vesicle destruction.[3,4,10] Some liposomes can also trigger the clotting cascade by binding to certain clotting factors in serum.[53] It was also found that fibronectin, immunoglobulins and C complement proteins catalyze interactions of liposomes with the cells of the RE system and/or activation of the complement system.[54] Minimal complement consumption was observed in rat serum by SUV containing 5 mol % ^{2000}PEG-DSPE.[55]

Most of the literature on the interactions of liposome with plasma components involves studies of the leakage of the entrapped material or stability in plasma in vitro or in vivo. However, only few studies of the adsorption of well-defined proteins exist.[56]

Although detailed studies have not yet been performed, several data show that the clearance of liposomes increases proportionally to the amount of protein bound onto liposomes. For instance, liposomes with 80 g of adsorbed protein per mole of lipid were found to exhibit half-life of a few minutes, these with 20–30 g/M, about 90–120 min, while liposomes with 5 g/M had a circulation half-life of 215 min.[56] It was also observed that liposomes which contain cardiolipin and phosphatidic acid bind more protein and are taken up quicker by the RES. On the other hand liposomes containing G_{M1} bind less protein and circulate longer than normal liposomes.[56,57]

In addition to these studies, which used poorly defined mixture of plasma proteins, interactions of several specific proteins with liposomes were also investigated. In addition to the binding of immunoglobulins,[58,59] liposomes were found to activate the complement as indicated by the adsorption of the C3 complement component.[60] In contrast, liposomes containing PEG 5000 were found to bind less proteins.[22]

Recently a method involving the photoaffinity cross-linking of plasma proteins with liposomes was introduced. While many of the results did not yield definitive answers, it was observed that the presence of PEG on the surface reduces the adsorption of large proteins which may otherwise bind to the phosphate group.[61] This is consistent with the reduced disintegration of PEGylated liposomes by phospholipases which was also reported.[62] Our preliminary data using black lipid membranes containing 5 mol % of ^{2000}PEG-DSPE also showed reduced interaction with proteins. Protein adsorption studied via surface pressure–molecular area changes of monolayers has not been performed yet.

In the previous section we have indicated that, besides interbilayer/interparticle steric stabilization, the intrabilayer cohesiveness, which reduces the kinetics of various interactions and exchange of liposomal molecules, can increase colloidal, physical, chemical, and biological stability of liposomes. These contributions will be reviewed in the next section.

4. Mechanical and Interactive Properties of Lipid Membranes

As discussed above, the most important design requirement for the long-circulating, nonleaking liposome is resistance to both degradation and immune recognition in the blood stream. In order to optimize the Stealth liposome design, we must choose the lipid bilayer composition and its grafted PEG polymer such that they promote or oppose the perceived mechanisms of degradation and uptake, depletion or

breaking away of PEG-lipids and PEG polymer, respectively.

As suggested by available in vivo data, we are looking for a particular set of material and interactive properties: bilayers should exhibit high mechanical cohesion while PEG chain should be grafted at appropriate density. Empirical data suggest that appropriate surface density is when polymer chains start to overlap. Obviously, the lipid system is more stable when polymer chains are not too long because this increases their aqueous solubility.[63] Distearoyl chains in distearoyl−cholesterol bilayer are probably the best lipid matrix for retaining the molecules within the bilayer. It was shown that at 8 h, for instance, 60% of the dose is still circulating in mice when DS was used as an anchor in DSPC/Chol bilayers as opposed to 35% for dioleoyl anchor and 20% for the control without PEG-lipids.[64] Increasing the hydrophobicity of the anchor to three palmitic chains did not result in any improvement while long-chained, saturated cardiolipins or other lipids with even more hydrophobic chains (such as Lipid A) and, eventually, bolaamphiphiles have not been tried yet. In the last case, however, the formation of liposomes may not be straightforward. The higher aqueous solubility of the PEG-conjugate is also the reason that PEG-cholesterols were found to be ineffective in prolongation of blood circulation.

To date, successes of the Stealth liposome, as will be described later have largely come from empirical developments, guided by rather qualitative features of liposomes and polymer-covered particles. What is needed now is a more quantitative approach. For example, the (PEG) polymer is clearly instrumental in providing the long-circulating liposome and it is widely believed that this is due to a steric stabilization barrier that opposes close approach of macromolecules and cells to the lipid bilayer surface. New measurements using X-ray diffraction,[66−69] surface force apparatus[70,34] (to be described later), and ellipsometric measurements of disjoining pressure as a function of osmotic pressure[71] are now addressing more quantitative issues regarding the distance the polymer layer extends from the bilayer surface, the compressibility of this barrier and how extension and compressibility change with PEG-lipid fraction in the bilayer and molecular weight. Also, if resistance to chemical/physical attack is of prime importance, then the more cohesive the surface is, the more likely it is to resist binding of other molecules (that involves some degree of intercalation into the lipid headgroup region) or direct solubilization by fatty solvents,[72,73] like lipoprotein particles. Again, direct measures of lipid bilayer compressibility modulus and failure,[72] when coupled with the in vivo data are showing how cohesive the bilayer has to be in order to maintain an acceptable degree of stability of structure and how this resistance can be enhanced by alloying the phospholipids with cholesterol.

Thus, from a colloidal force and materials points of view, the two basic physical properties that have emerged as being of fundamental importance to liposome stability and overall protective effect are the size and compressibility of the polymer layer, and the cohesion of the lipid bilayer matrix itself. We will review some recent experimental measurements and theoretical models that have begun to give the Stealth engineer the necessary data from which to select appropriate materials with which to match the emerging definition for "operating conditions in service".

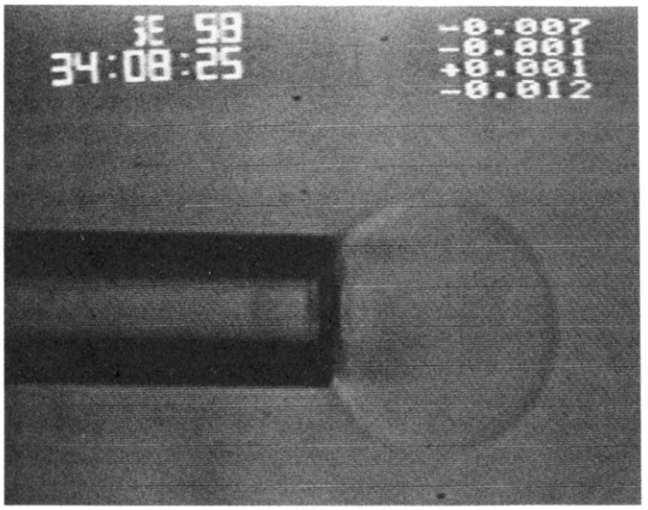

Figure 7. Videomicrograph of a single liposome (30 μm diameter) in a suction micropipet (8 μm diameter). Using this micropipet manipulation technique, we can determine the elastic behavior and mechanical strength of the lipid bilayer, as well as bilayer permeability to water and encapsulated drug.

4.1. Bilayer Elasticity and Mechanical Failure: Micropipet Manipulation

Although many spectroscopic and calorimetric methods give a wealth of information concerning the molecular conformation and motion of bilayer lipids (from which bilayer material properties must originate), the most reliable indicator of membrane material properties is from direct mechanical measurement. While some methods are based on osmotic swelling of vesicles,[74] the method of choice is the micropipet manipulation of individual, giant (20 to 40 μm diameter), unilamellar vesicles.[47,75−79,72] Given that the lipid bilayer is only two molecules thick, special optical and mechanical methods have been developed in order to make such direct measurements. The interference contrast optics can be enhanced by making the vesicle internal solution (sucrose) of different refractive index to the external media (glucose or NaCl). The suction micropipet acts not only as a means of applying a well-prescribed force to the vesicle, but, in the compressibility and failure experiments, it also acts as a sensitive transducer of membrane area changes that can be as small as 1−5%.

The videomicrograph in Figure 7 shows a lipid vesicle that is being manipulated by a suction micropipet. The internal pipet diameter is 8 μm and the vesicle diameter is 30 μm. In this experiment the liposome is pressurized by the suction pipet and this induces an isotropic tension in the membrane and a corresponding expansion in membrane area, which corresponds to an increase in the projected area per molecule of the constituent lipids. The eccentric behavior of individual molecules in the

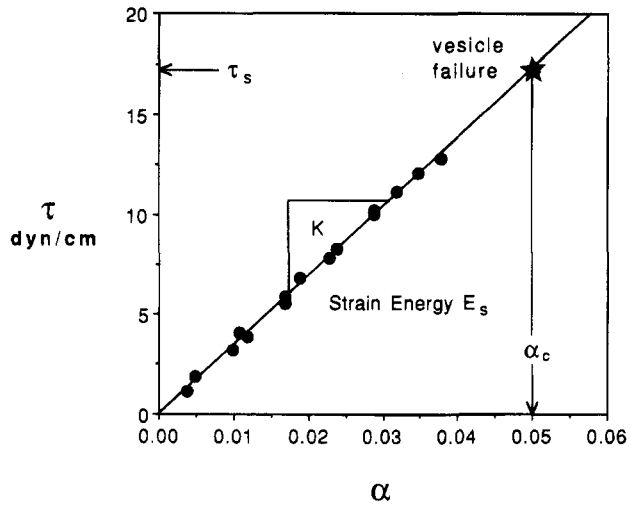

Figure 8. Stress vs strain plot for micropipet pressurization of a lipid vesicle composed of SOPC/cholesterol (2/1) (Needham and Nunn, 1990). Vesicle membrane tension τ resulting from the applied micropipet suction pressure is plotted versus the areal strain α (i.e., the observed increase in vesicle membrane area ΔA relative to an initial low stressed state A_0). The slope of the τ vs α plot is the elastic area compressibility modulus K. The star symbol represents the point of membrane failure at the critical areal strain α_c and tensile strength τ_s. The area under the plot represents the strain energy at membrane failure E_S.

plane of the membrane is, of course, averaged out and we can only view the membrane as continuum in the surface plane. Across the thickness of the bilayer, molecular features are clearly dominating.

As Evans has shown[80] the thermodynamic changes that result from membrane deformation and rates of deformation provide constitutive relations for membrane material properties. Thin shell membranes can be deformed in one or a combination of three ways: area expansion, elongation, and bending. In the membrane compressibility experiment, the area dilation mode of deformation is isolated. A simple relation between membrane tension T and change in area A relative to an undeformed area A_0 characterizes the area elasticity in terms of an isothermal area compressibility (expansivity) modulus K:

$$K = \Delta T/(\Delta A/A_0)$$

In the micropipet measurement, the membrane is sequentially loaded and unloaded by increasing and decreasing the pipet suction pressure and the corresponding changes in the projection length in the pipet are measured. A final increase in the suction pressure produces failure. The membrane tension is derived from the suction pressure and pipet and vesicle geometry. The area change, at constant vesicle volume, is related to the length change of the membrane projection in the pipet.[77]

As shown, in Figure 8,[72] all the deformation up to failure is elastic (the motions of molecules are on the order of microseconds for this liquidlike membrane and so viscous effects are not observable[80] and the lipid membrane can be characterized in terms of four material parameters:

1. Membrane area compressibility represents the resistance of the membrane to isotropic area dilation and is characterized by the isothermal area compressibility or expansion modulus K.

2. Critical areal strain is the fractional increase in membrane area at failure α_c.

3. Tensile strength is given by the membrane tension at lysis (rupture) τ_{lys}.

4. Membrane strain energy (or toughness) E_S represents the work done on the membrane up to failure and is given by the area under the stress strain plot $K(\alpha_c)^2/2$. It can be converted to energy/mole by knowing the area/molecule.

These material parameters have been measured for a range of lipid types and lipid/cholesterol mixtures.[47,72,77-81] Some of the data is presented in Table 2. With reference to the stability of drug delivery liposomes, it is important to note the low area expansivity (high expansion modulus) and high strength conferred by the inclusion in the bilayer of saturating levels (ca. 50–55 mol %) of cholesterol; cholesterol is by far the most effective way to increase bilayer cohesion. Interestingly, strain energy is a maximum for intermediate (ca. 40 mol %) levels of cholesterol. Cholesterol exerts its effect via an ordering of the lipid molecule (especially in the outer regions of acyl chains) while still maintaining a liquidlike interior due to a disruption of long-range order.[82,83] It therefore forms a liquid ordered phase with phospholipids over a wide temperature range.[82,83]

Several features of the relation between lipid bilayer cohesion and lipid composition have emerged from these studies. The disordering effect of many double bonds per chain is shown by considering the lipids, DAPC and SOPC (diarachydonoyl phosphatidylcholine and stearoyl oleoyl phosphatidylcholine). As shown in Table 2, the lipid with the most chain disorder, DAPC, showed a correspondingly lower elastic modulus and tensile strength than SOPC—the lipid with only one double bond in one of its acyl chains.

As can be seen from the stress vs strain behavior (Figure 8), liquid lipid membranes always fail without exhibiting any ductility and so the strain energies also reflect the difference in strength between the two membranes. These energies should also be equivalent to the free energy of bilayer expansion due to adsorption of any molecule into the headgroup region of the bilayer.[84] Coupling these two parameters in adsorption experiments should give more mechanistic information regarding the interaction of blood components with the liposome surface. Again the micropipet method should provide sensitive measures of adsorptive interactions that increase area per molecule on the order of a few percent.[72,85]

With regard to the effects of cholesterol, area expansion modulus K vs nominal mole % cholesterol in the lipid bilayers for several lipid/CHOL mixtures are shown in Figure 9. As the amount of cholesterol in the SOPC lipid bilayer is increased the elastic modulus shows little change initially but then increases rapidly. At just less than 60 (nominal) mol %, the property saturates and this reflects the chemical saturation of cholesterol in the bilayer phase. (Any excess cholesterol that might be included in the initial lipid/cholesterol sample from

Table 2. Cohesive Properties of Vesicle Bilayer Membranes Containing Cholesterol[a-c]

lipid system	mol %[b]	K (dyn/cm)	α_c	τ_s (dyn/cm)	E_s (J/mol)	A_m (calcd) (Å^2)
DMPC		140				
DLPC/CHOL	50	1200				
DMPC/CHOL	50	2575				
DPPC/CHOL	50	2235				
DSPC/CHOL	50	3278				
DArPC/CHOL	50	4269				
SOPC	0	193 ± 20	0.030 ± 0.004	5.7 ± 0.2	34 ± 9	65.0
	14	216 ± 12	0.041 ± 0.009	8.7 ± 1.8	65 ± 29	59.1
	28	244 ± 24	0.051 ± 0.012	12.6 ± 2.7	106 ± 46	53.2
	38	333 ± 9	0.051 ± 0.009	16.9 ± 3.2	132 ± 52	49.0
	43	609 ± 44	0.031 ± 0.004	18.4 ± 2.9	79 ± 13	46.9
	43	568 ± 36	0.031 ± 0.002	17.8 ± 1.8	86 ± 20	46.9
	48	710 ± 48	0.029 ± 0.005	20.6 ± 3.7	83 ± 30	44.8
	50	781 ± 45	0.025 ± 0.004	19.7 ± 3.2	64 ± 25	44.0
	53	907 ± 73	0.023 ± 0.002	19.4 ± 2.2	57 ± 9	42.7
	58	1207 ± 135	0.022 ± 0.002	24.9 ± 2.1	72 ± 10	41.9
BSM	50	1718 ± 484	0.016 ± 0.004	23.2 ± 5.9	49 ± 14	40
SM/CHOL	50	1799				
22:12PC/CHOL	50	1721				
DAPC	0	57 ± 14	0.036 ± 0.014	2.3 ± 0.6	19 ± 11	80
	50	102 ± 24	0.043 ± 0.010	4.5 ± 0.6	32 ± 10	58.5

[a] Material property parameters for lipid vesicle bilayer systems at 15 °C composed of a variety of lipid types and lipid/cholesterol compositions (Needham and Nunn, *Biophys. J.* **1990**, *58*, 997, and D. Needham Cohesion and Permeability of Lipid Bilayer Vesicles. In *Permeability and Stability of Lipid Bilayers*; Disalvo, E. A., Simon, S. A., Eds.; CRC Press: Boca Raton, FL, 1995; pp 43–76). Shown are the elastic area compressibility modulus K, the critical areal strain α_c, the tensile strength τ_s, and the strain energy E_S. The last column gives the calculated average area per molecule A_m (calcd) for each bilayer system and composition according to a simple stoichiometric model. The reduction of A_m with addition of cholesterol indicates its condensing effect. [b] Mol % is nominal concentration of cholesterol in original chloroform solution from which vesicles were made. [c] Abbreviations: PC, phosphatidylcholine; CHOL, cholesterol; DAPC, diarachidonylphosphatidylcholine; DMPC, dimyristoyl phosphatidylcholine; SOPC, stearoyloleoylphosphatidylcholine; BSM, bovine sphingomyelin; SM, synthetic sphingomyelin; DLPC, dilauroyl phosphatidylcholine; DPPC, dipalmitoyl phosphatidylcholine; DSPC, distearoyl phosphatidylcholine; DArPC, diarachidoylphosphatidylcholine.

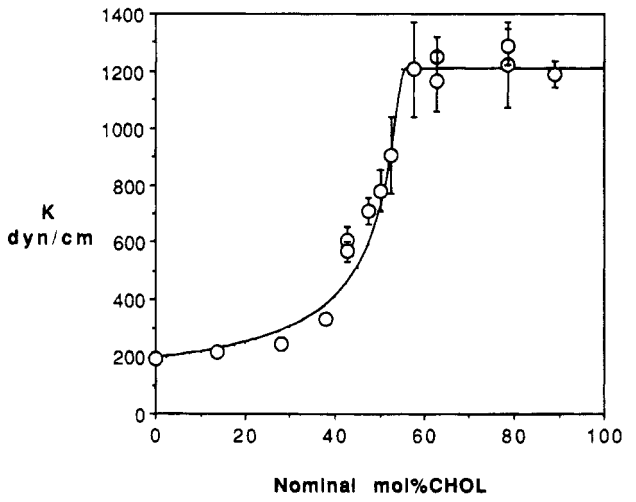

Figure 9. Area expansion modulus K vs nominal mole % cholesterol in SOPC lipid bilayers. The elastic modulus reaches a maximum when excess cholesterol saturates the bilayer phase at concentrations greater than 60 mol %. Also shown is a comparison between experimental membrane modulus and a molecular composite model (solid line) (Needham and Nunn, 1990).

which the membranes are made is present in aqueous suspension as a separate cholesterol crystallite phase.)

Interestingly, the elastic modulus of RBC lipids with 40 mol % native cholesterol is on the "calibration curve" given by the SOPC "standard". So, in this material property test, the acyl chain composition of a single lipid is equivalent to natural lipid mixture that averages out to the same 18:0/18:1 composition, i.e., SOPC behaves to a first approximation like many natural membranes, even though natural membranes are composed of several lipid types containing acyl chains of various degrees of length and unsaturation.

The nonlinear behavior of this elastic property has been modeled by a simple form of composite theory[72] which views the lipid membrane as analogous to particulate composite that is loaded in an Iso-stress mode. The two components, free lipid and lipid that is strongly coupled to cholesterol, each brings to the molecular composite bilayer its own elastic behavior through neighbor interactions that are averaged out according to simple mixing relations. It is assumed that, during isotropic loading of the membrane composite, the stresses in the two components are equal and continuous across molecular boundaries between them, and that the total strain is a linear combination of the strains of each component multiplied by their respective area fractions. This relation between experimental membrane modulus and molecular composite model is also plotted in Figure 9 and matches the nonlinear increase in bilayer area expansion modulus with increasing mole % cholesterol. Thus, a simple property-averaging theory can account for the nonlinear increase in area modulus that is observed when the mole % of cholesterol in the bilayer is increased.

From these measurements on a range of lipid and lipid/cholesterol mixtures, the underlying feature of bilayer compressibility is that compressibility decreases with decreasing area per lipid molecules and depends on how close the lipid is to its limiting area per molecule (~40 Å^2). Whether lipids are condensed by attractive interactions with cholesterol or by reduced relative temperature (relative to their pure gel–liquid crystalline phase transition temperature), the effect on the compressibility of the bilayer is the same. Thus, while the hydrophobic effect can be responsible for the assembly of lipids in aqueous

Table 3. Blood Circulation Half-Lives and Some Physical Parameters of Noncharged and Surface Unmodified Liposomes with $2r \sim 100$ nm[a]

A. Unsaturated RES

RES	$t_{1/2}$ (min)	RES	$t_{1/2}$ (min)
PC	<6	DSPC	20
PC/Chol (2:1)	30	DSPC/Chol (2:1)	100
PC/Chol (1:1)	40	DSPC/Chol (1:1)	>120

B. Saturated RES

RES	$t_{1/2}$ (h)	RES	$t_{1/2}$ (h)
EPC	<0.1	EPC/Chol (1:1)	2
hydrogenated EPC	1.3	DMPC/Chol (1:1)	6
DSPC	1.5	DPPC/Chol (1:1)	12
DLPC/Chol (1:1)	0.1	SM/Chol (1:1)	16
DOPC/Chol (1:1)	1.1	DSPC/Chol (1:1)	20

[a] The $t_{1/2}$ values are rather approximate. The data in the literature are rather confusing: most of the studies do not pay attention to the RES saturation and the reported data are of low general value. As an extreme example we should mention liposomal blood substitutes which are administered at extreme doses, up to 100% blood substitution and in which virtually any kind of stable liposome can have $t_{1/2}$ in the order of days. Also different markers are used and often unrealistic statistical analyses are applied which can give overestimates due to the monitoring of the marker in β and γ phases while the liposome uptake occurs in the α phase. Data for A are obtained from refs 13 and 25, and for B from ref 13. These studies report mostly long circulation times and the formulations tested are controls and resolutions in the graphs are very low.

media and sets the lower limit on the compressibility, there appears to be additional bonding forces especially in phospholipid/cholesterol mixtures responsible for bilayer integrity. These high modulus membranes are now showing material behavior similar to other physically bonded materials like high-density polyethylenes where the repulsive (thermal) forces are counteracted by the attractive, in this case, van der Waals, forces between molecules.

These recent experiments have shown that the lipid bilayer is a cohesive material whose elasticity can be made to range by a factor of almost 100 depending on lipid type and lipid/cholesterol composition. Compare this behavior with that of metals, where lead to tungsten is not quite 20 times and for ceramics, ice to diamond just about makes 2 orders of magnitude. The bilayer shows a very wide range of elasticity for any single type of material; never mind a structure that is only two molecules thick.

Furthermore, these measurements can qualitatively explain numerous empirical data collected in a variety in vitro and in vivo assays (some of them are shown in Table 3) with many different lipid compositions (compare Table 2 and 3). Figure 10 shows data from Table 3 plotted as a function of elastic modulus. Despite different experiments and saturation of RES, the blood circulation times still show qualitative agreement with membrane mechanical properties. While significant improvements in mechanic properties come after 40 mol % cholesterol, a reduction of the uptake commences already at 30 mol % cholesterol and plateaus thereafter. At present we can only speculate that adsorption of opsonins can be prevented already at moderate levels of membrane cohesion. In addition, by using these arguments, permeability characteristics of liposomes in "test tube" experiments can be explained. PEG

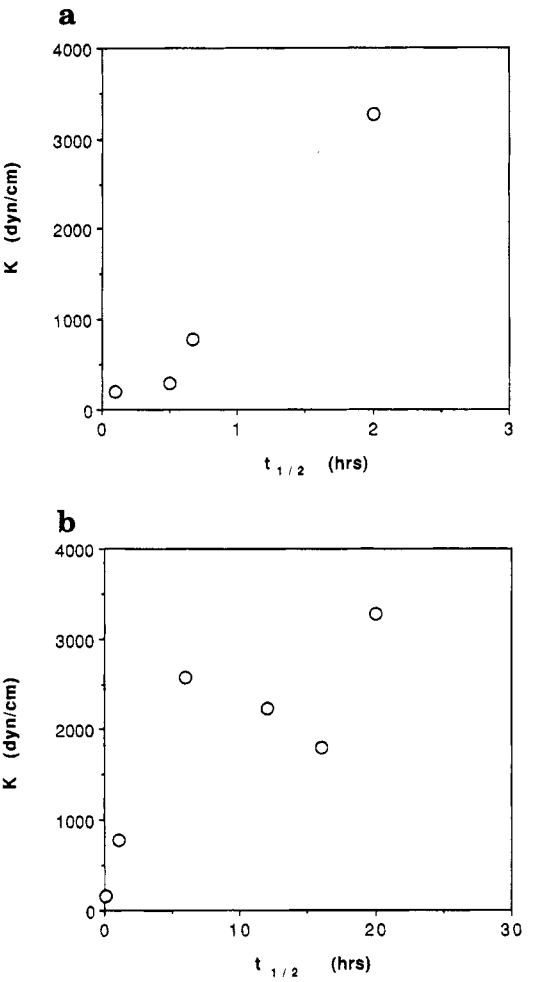

Figure 10. Blood circulation times of conventional liposomes, as adapted from ref 13 (and Table 3) as a function of membrane elastic modulus: (a) data for the unsaturated RES and (b) data from the case of saturated RES.

chains above the bilayer, however, are also expected to influence the cohesivity of the bilayer.[69,85]

4.2. Interbilayer Interactions: X-ray Diffraction and Micropipet Manipulation

In recent experiments and theoretical tests of interaction potentials it has become clear that the lipid bilayer provides a unique system for the study of a range of colloid and surface phenomena at and between surfaces. The ability to deal with equilibrium structures is of great necessity when we are considering equilibrium properties. In this regard, unlike solid biomaterial surfaces the lipid bilayer can be in a liquid state.

In order to determine forces of interaction between bilayers and other surfaces, the planes of origin have to be clearly defined experimentally as well as theoretically, and the scale of surface roughness should be less than the range of intersurface forces. In this regard, the lipid bilayer provides an essentially molecularly smooth surface, although observations of molecular scale surface roughness effects are now being made in systems composed of lipids with different sized headgroups and states of rigidity.[86-90] For solid materials, only atomically smooth mica sheets can provide clean reproducible surfaces in the crossed cylinder microbalance.[91,92]

The liquid nature of the membrane promotes homogeneity of composition at the molecular scale, and moreover, the self-assembly of lipids ensures control over cleanliness and reproducibilty of structure. Whereas the evenness of chemical polymer grafting depends on the cleanliness and homogeneity of the solid plastic, glass, metal, or other such biomaterial, the expression of polymers (as lipid-bound polymer) at the lipid bilayer surface relies only on the physical self-association between compatible lipids. Also, by judicial choice of lipids and other membrane compatible components, the lipid surface can be made to be neutral or charged (positive or negative), poorly or highly hydrated, and bare or polymer covered. Appropriate choice of lipid acyl chain composition allows the surface structures to be mobile in a fluid substrate or immobile in gel-state lipids. Finally, specific surface groups of special relevance to cell adhesion and surface recognition such as receptors, antigens, or antibodies can be coincorporated with PEG-lipid into the lipid bilayer for controlled reconstruction studies in which background adsorption is eliminated.[49]

Lipid bilayer membranes in aqueous media interact nonspecifically via electrostatic, and solvation forces, commonly recognized as van der Waals attraction, electric double-layer repulsion, and hydration repulsion.[91–98] Other steric and structural interactions exist that are currently being defined, such as the very short range steric interaction,[86–90] and a weak opposition to formation of adhesive contact due to thermally driven bending undulations of the ultrathin membrane.[81] As a complement, and possibly supplement, to hydration forces, repulsive protrusion forces were recently introduced.[99]

The most direct approach to understanding interactions would be to measure simultaneously the individual forces of interaction and the corresponding distance between surfaces.[100] This force vs distance approach[101] has been very successful for interactions between mica sheets and other solid materials as crossed cylinders. Later, the force balance technique was adapted to study interbilayer forces[102–104] for supported bilayers deposited and attached to the solid mica substrates. In this approach, forces are cumulated with distance to give the overall interaction potential.

Another approach was conceived of by Evans in which the interfacial free-energy density for the adhesion of unsupported lipid bilayers as vesicles could be measured using a micropipet manipulation method.[105] Vesicle manipulation techniques were developed and a series of experiments were carried out that measured mutual adhesion energies for bilayers that exhibited a range of colloidal interaction potentials.[47,75,76,105–110] Here, we will briefly discuss the vesicle adhesion test using a micropipet.

4.2.1. Vesicle–Vesicle Adhesion Experiment

As shown in Figure 11[47] the vesicle on the right, in the holding pipet, is under high suction pressure (10 000 dyn/cm^2) and forms a rigid, spherical test surface, while the vesicle on the left, in the measuring pipet, is under lower (starting pressure of ~1000 dyn/cm^2), variable suction pressure and remains deformable. The vesicles are aligned and maneuvered into close proximity and the pipets are maintained in these fixed positions so that no axial force is exerted during the adhesion test. The extent of adhesion is then controlled via the tension in the left-hand adherent vesicle membrane, which in turn is controlled by pipet suction pressure.

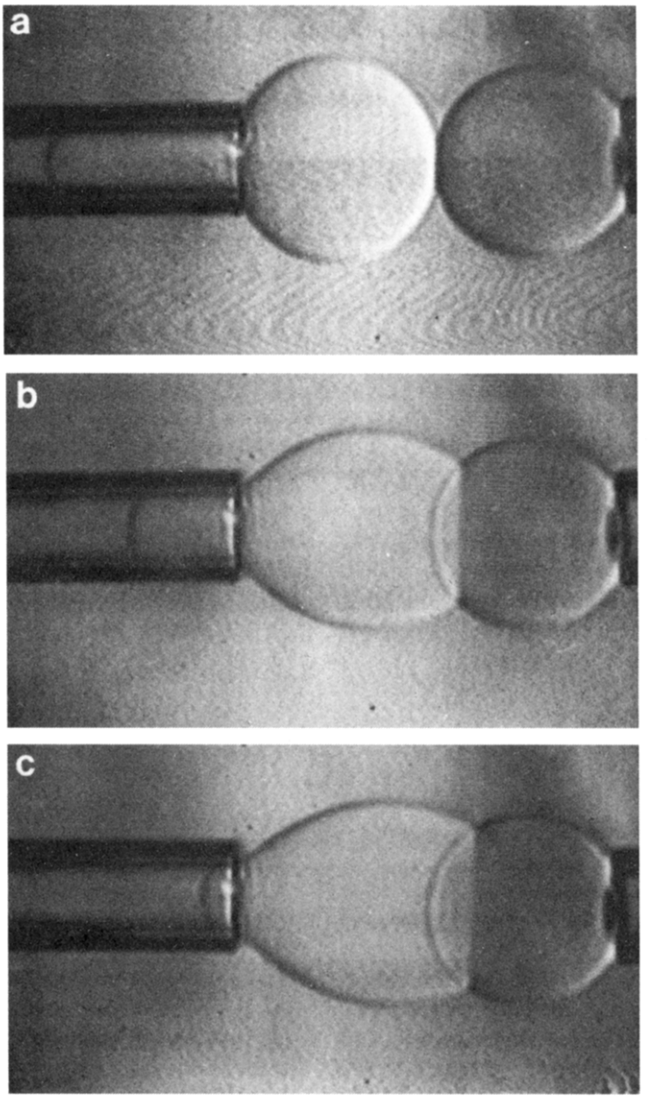

Figure 11. Video micrographs of liposome adhesion test between neutral (SOPC) lipid bilayers in which liposome membrane tensions and the extent of adhesive spreading are controlled by pipet suction pressures (Evans and Needham, *J. Phys. Chem.* 1987): (a) The liposome on the right (25 μm diameter) is held under high tension (~3 dyn/cm) so that it forms a rigid spherical test surface. The liposome on the left is held under lower, variable suction pressure. The liposomes are maneuvered into close proximity but not forced into contact and the pipets are then left in these fixed positions. (b) and (c) Spontaneous adhesion is allowed to occur in discrete, equilibrium steps controlled by pipet suction pressure applied to the left-hand liposome. The adhesion energy is calculated from the pipet suction pressure and pipet and liposome geometries.

The reversible work of adhesion ω'_a to assemble bilayer surfaces is the reduction in free energy per unit area of membrane–membrane contact formation.[80,81] It is the cumulation of the action of densely distributed interbilayer forces from large separation (infinity) to intimate contact. Mechanical equilibrium at stable contact is the balance between the free

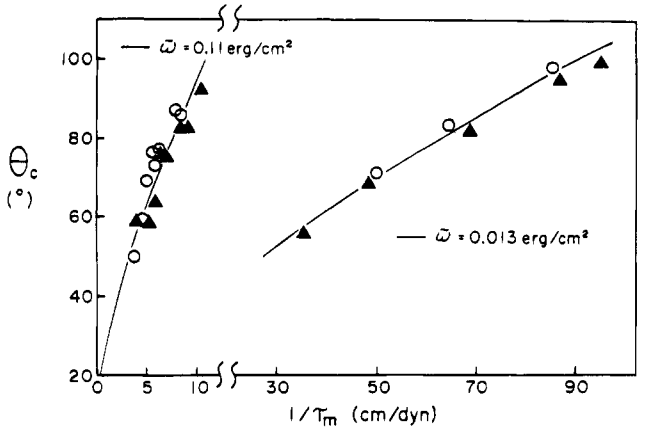

Figure 12. Each discrete, equilibrium step in the adhesion and peeling experiment (closed triangles represent contact formation and open circles represent separation of contact) is analyzed to yield a plot of extent of encapsulation of the rigid vesicle surface x_c vs reciprocal suction pressure P multiplied by pipet radius R_p. With values for vesicle area and volume determined prior to the adhesion experiment, plus mechanical analysis of membrane geometry, measurements can be converted into precise contact angles vs the reciprocal of membrane tension for the adherent vesicle. Solid curves are predictions for uniform-fixed values of free energy reduction per unit area of contact formation. Two cases are shown representing the operation of two different long-range forces: van der Waals attraction $\omega_a \sim 10^{-2}$ erg/cm^2) and depletion attraction in a concentrated solution of nonadsorbent dextran polymer ($\omega_a \sim 10^{-1}$ erg/cm^2).

energy required to increase contact area and the mechanical work to deform the vesicle contour, and is represented by the Young/Dupre equation:

$$\omega_a = \tau_m (1 - \cos \theta_c)$$

where τ_m is the membrane tension in the adherent vesicle and θ_c is the included angle between the adherent and test surface membranes exterior to the contact zone. Thus, for constant adhesion energy, a unique relation exists between membrane tension and contact angle for the membrane assembly experiment. The contact angle can be derived from measurements of the extent of encapsulation x_c of the spherical test surface because there exists a precise relation between x_c and θ_c for fixed vesicle area and volume, determined prior to adhesion.[81,105,106] Membrane tension is calculated from the pipet suction pressure ΔP and vesicle and pipet geometry:

$$\tau_m = \Delta P R_p / 2(1 - R_{p/c})$$

where R_p is the pipet radius and c is the mean curvature [$c = (1/R_1 + 1/R_2)/2$)]. A first approximation would take the vesicle surface as a perfect sphere of radius R_0 and c would then equal $1/R_0$. Otherwise, mean curvature must be established from the geometrical requirements imposed by the fixed distance between the pipets and the fixed surface area and vesicle volume.[105]

Thus, for a given vesicle pair, both adhesion and separation can be represented by a plot of contact angle vs reciprocal membrane tension for the adherent vesicle membrane, and a single value of the adhesion energy is then used to fit the experimental data Figure 12. Two cases are shown representing the operation of two different long range forces: van der Waals attraction ($\omega_a \approx 10^{-1}$ erg/cm^2) and depletion attraction in a concentrated solution of nonadsorbing dextran experiment.[47,110]

The above analysis relates to a regime where the adhesion energy is strong enough such that edge energy effects due to membrane bending and random thermal undulations are insignificant. This strong adhesion regime starts at the very limit of experimental measurement using the micropipet method, i.e., for adhesion energies greater than 10^{-3} erg/cm^2. The technique has therefore been successfully used to measure the cumulated energy for a whole range of interbilayer interactions (van der Waals attraction, short hydration repulsion, electrostatic double-layer repulsion, and attraction induced by the presence of nonadsorbing polymer) that result in stable adhesive contact.[47,111,81]

4.2.2. X-ray Diffraction

There are however, two parts to the problem of characterizing interactions when forces and distances of separation are not measured simultaneously. One part, as discussed above, is the measurement of the resulting adhesion energy and the other is a measurement of the distance of equilibrium bilayer separation at contact and the contribution of repulsive potentials to the total interaction potential. The distance parameter and repulsive potential information has been provided by X-ray methods using multilamellar lipid preparations that measure a repeat period which can be divided up into bilayer thickness and interbilayer gap separation.[81,88-90,94-96,111-116]

In a series of experiments carried out by McIntosh et al., the dimensions of the lipid bilayer and the intervening fluid space are determined from electron-density profiles.[94] Figure 13 shows the familiar electron-dense peaks representing the location of the lipid headgroups, the low-electron-dense trough in the middle of the bilayer where the terminal methyl groups are located and the intermediate density regions between bilayers that is the water-filled interbilayer fluid space.

These methods not only give equilibrium contact distances but also allow pressures to be applied that force the interaction up the repulsive part of the free-energy minimum and thereby allow repulsive contributions to be directly measured. The method is also useful because during these compressions of the interbilayer gap, the geometry of the lamellae (bilayer thickness) and phase behavior of the lipids can be monitored. The two profiles in Figure 13 are for a phosphatidylcholine (PC) bilayer system at zero applied pressure and under an applied pressure of 57 atm.

At zero applied pressure, the bilayers are in a van der Waals minimum at ~15 Å separation, and as the applied pressure is increased (by equilibrating the multilamellar lipid preparations with large polymer osmoticants[94]) the interbilayer space is seen to decrease, while the bilayer thickness remains essentially unchanged. Furthermore, the relationship is exponential and the decay constant is on the order of the size of the water molecule ~2 Å. At extremely high pressures the slope changes when practically all

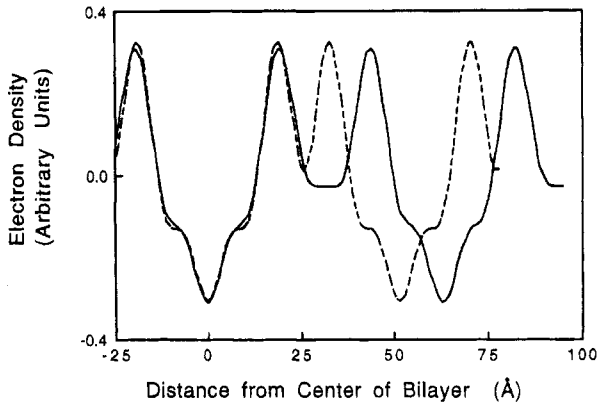

Figure 13. Electron density profiles for PC bilayers. The high electron density peaks are the lipid headgroups and the lower density regions are the hydrocarbon chains, with the lowest density representing the terminal methyl groups in the center of the bilayer. The medium density region between the bilayers is the interbilayer aqueous space. Starting from zero applied pressure, with the bilayers (in a van der Waals minimum) at ~15 Å separation, pressure can be applied to the system, by equilibrating the multilamellar lipid preparation with large polymer osmoticants, and the amount of water of hydration can be competed for. In doing this the interbilayer space is seen to decrease as higher pressures are applied. The bilayer thickness or structure does not change upon compression and the decrease in repeat period is essentially all due to decreasing the water gap. Applied pressure: (—) 0 atm and (- - -) 57 atm.

of the water of hydration has been removed and the headgroups come into very close steric interaction.[88]

It is from these kinds of measurements that the structural and interactive properties of many bilayer systems have been characterized. At this point it is useful to note that we are dealing with a bilayer that can be treated as a 30–35 Å thick hydrocarbon layer plus a hydrophilic headgroup that adds on another ~10 Å. Interbilayer gaps can range from 3 Å up to 50 Å at which point the diffraction patterns become somewhat diffuse and difficult to analyze. Thus, the graininess of matter should be exposed at these dimensions, yet continuum theories of attraction and repulsion have been used to model and match the experimentally observed data. In these approaches then, the equilibrium separation distance and the net free energy of adhesion can be combined to test interaction potential laws.

Before we discuss how the presence of surface polymer prevents the operation of underlying attraction between bilayers, it is useful, as a way of calibrating our understanding of interbilayer interactions, to first discuss the nature of interactions in the absence of grafted polymer.

4.2.3. Interbilayer Interactions: Neutral Bilayers

For neutral bilayers it is expected and found that the interaction involves van der Waals attraction that is ultimately limited by hydration repulsion. Compared with liquid–liquid contact energies (characterized by near atomic contact) which are ~100 erg cm^{-2}, free energies for interbilayer adhesion have been measured by micropipet methods to be ~10^{-1} erg cm^{-2}.[47,107–109] For adhesive contacts that are stabilized by other repulsive forces such as electrostatic and undulation repulsion, adhesion energies can be less than 10^{-3} erg cm^{-2}.[75,76] These small values are apparently due to the relatively large separation between bilayers at stable contact in contrast to near-atomic distances characteristic of liquid–liquid cohesion.

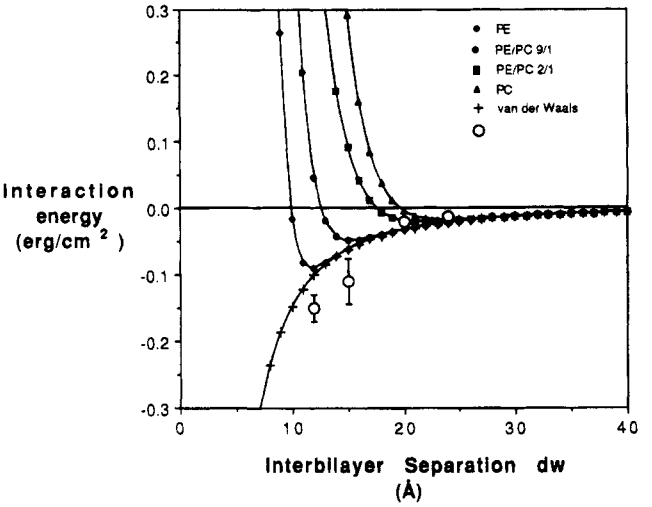

Figure 14. Total interaction potentials calculated for PC, PE, and PC/PE systems (small closed symbols) and the van der Waals attraction potential (cross). Data from adhesion energy measurements on the same bilayer systems is also shown (large open circles).

van der Waals Attraction: Separated by a medium with different polarizing properties, bilayers are drawn together by long range van der Waals forces.[98,91] The form of the interaction potential for two semi-infinite slabs is

$$\Phi = -A_H \cdot f(d_w/d_b)/(12\pi d_w^2)$$

where A_H is the Hamaker coefficient and d_w is the water-gap thickness. $f(d_w/d_b)$ is weak retardation function of the ratio of the bilayer thickness d_b to the distance between bilayers. Thus, the attractive approach to adhesive contact is along a "soft" attraction potential that increases as $1/d_w^2$.

4.2.4. Steric and Hydration Pressures

At short distances on the order of only a few angstroms, structure and solvation forces associated with the lipid headgroups and the intervening solvent dominate repulsion for all lipids. X-ray diffraction studies of forced dehydration (by osmotic or mechanical stress) of multilamellar lipid–water phases show that the short-range repulsion follows a steep exponential decay λ_{sr}:[95–97]

$$F^{sr} = \lambda_{sr} P_{sr} \exp(-d_w/\lambda_{sr})$$

The cumulated interaction potential for neutral bilayers is therefore given by

$$F_T = \lambda_{sr} P_{sr} \exp(-d_w/\lambda_{sr}) - A_H \cdot f(d_w/d_b)/(12\pi d_w^2)$$

As shown in Figure 14, total interaction potentials can be plotted for neutral bilayers. The parameters λ_{sr} and P_{sr} have recently been measured, using an X-ray method.[117] The van der Waals attraction always starts out at a larger separation distance than

the hydration repulsion, which comes in very steeply in shorter range, and so neutral bilayers always exhibit attractive force among themselves. As is clear from the cumulated interaction, the free-energy potential for assembly of neutral bilayers to stable contact essentially represents the attractive van der Waals potential at the final separation distance. If we now compare this semiempirical theory with adhesion[118] data we see that the combination of these two techniques (micropipet manipulation and X-ray diffraction) come fairly close to testing these continuum theories down to the several angstrom size range!

4.2.5. Neutral Bilayers and the Influence of Thermal Undulations

Lipid bilayers can have very small bending stiffness, only a few kT, and so "flap around in a thermal breeze" like "bed sheets on a washing line". Soft repulsion is predicted for thermally excited bending undulations in unsupported bilayers.[119] The origin of this repulsion lies in the work required to drive heat out of the system as the bilayers are forced together. Two regimes can be identified.

(i) For separations less than equilibrium contact, the primary effect of bilayer undulations is the observed decay length for short-range repulsion and expand the separation at full hydration for unsupported membranes. For immobilized lecithin bilayers it is predicted that the adhesion energy would be 4−5 times larger than that measured for unsupported bilayers because of the removal of this short-range fluctuation repulsion. Stronger adhesion has in fact been measured for lecithin bilayers adsorbed on mica sheets.[92]

(ii) At distances well beyond equilibrium separation, the free-energy excess from thermomechanical excitations of the lipid bilayers is predicted to follow a weak steric repulsion given by

$$F_{fl} = c(\pi kT/16)^2/(Bd_w^2)$$

where B is the bilayer curvature elastic modulus and $c \approx 5$.[119]

For neutral bilayers, this weak steric repulsion does not overcome the van der Waals attraction at close separations while at large separations (about 100 Å), the repulsive stress is predicted to be small and that this repulsion is insignificant for most phospholipid membranes. Of course, this undulation force exists also between charged bilayers. Charge as well as surface polymer may stiffen the bilayer and reduce this force.

4.2.6. Charged Bilayers

A series of experiments were carried out that studied PC/PS mixtures of 0−10 mol % PS[47] and it was shown that the presence of negative charges in the bilayer surface produces a larger range repulsion force that attenuates the adhesion energy due to van der Waals forces. These negative charges are simply introduced by incorporating negatively charged lipids such as phosphatidylserine or phosphatidylglycerol, both having one net negative charge per molecule,

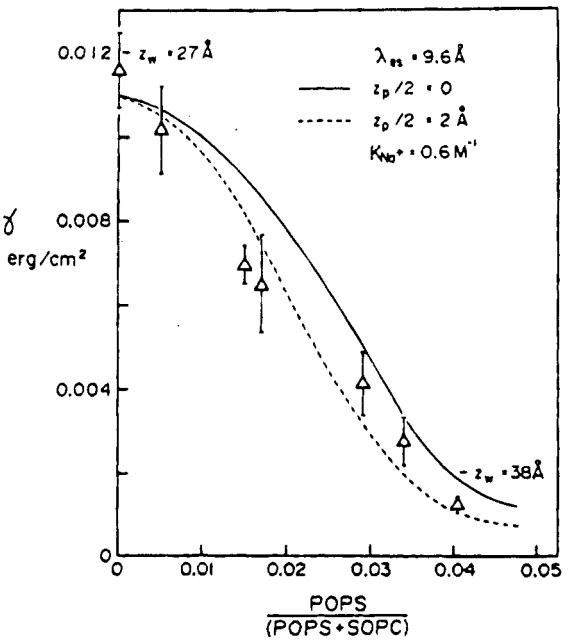

Figure 15. Adhesion energies measured by micropipet manipulation for mixed PC/PS bilayers in 0.1 M NaCl. The adhesion energy is attenuated and the van der Waals attraction is overcome when bilayers contain ~5 mol % negative lipids. Solid and dashed curves are predictions of electric double-layer theory.

into a bilayer composed mainly of neutral lipids such as phosphatidylcholines.

The limited electrostatic double-layer potential for repulsion between two charged plates in an electrolyte can be shown to be

$$F_{es} = \kappa^{-1}64n_0kT\psi_0^2 \exp(-d_w/\kappa^{-1})$$

where n_0 is the number of charged ions per cubic centimeter; Ψ_0 is a parameter that is related to the surface potential σ_0, which for 5 mol % PS is ~0.021 V (the corresponding Ψ_0 value is 0.1968); d_w is the distance between the bilayers assuming them to be infinite plates; κ^{-1} is the double layer thickness, 0.96 × 10^{-9} m for a concentration of 100 mM NaCl.

This interaction therefore has the same exponential form as the hydration repulsion but its large decay constant (~10 Å) means that at 5 mol % negative charge the repulsion will dominate and the bilayers are stabilized against adhesion[47] as predicted by double-layer theory. Interbilayer adhesion energy measurements are plotted for the PC/PS system as a function of PS mol fraction in 100mM NaCl in Figure 15 and support this cumulation of potentials.[47]

Thus, ideal double-layer theory works well at this separation of ~3 Debye lengths (κ^{-1} = 9.6 Å in 0.1 M NaCl) and the results are consistent with the combined distance dependence of attraction and repulsion. Given this effective repulsive potential the liposome engineer might ask "if small amounts of surface charge produce significant repulsions then why doesn't surface charge make liposomes Stealthy?" Presumably positive−negative, charge−charge interactions during opsonizaton and phagocytosis override any mutual colloidal stability that might have prevailed between negatively charged surfaces. Thus, it is not possible to provide a repulsion by double-

layer potentials in biofluids. This brings us to the importance of grafted polymer and its role as a stability barrier. Essentially, steric stabilization provided by grafted polymers is the only effective nonspecific repulsion for these kinds of biosurface/biofluid interactions.

4.2.7. Polymer-Grafted Liposomes

The liposome design engineer has only to look to the natural membrane itself to find a biosurface system which he/she might mimic in order to create an immunologically invisible or "Stealth" liposome. Electron micrographs of the surface of a red blood cell[120] show that it is covered by a molecular "fuzz" or glycocalyx, an unusually "lush" 140 Å thick coat of oligosaccharide filaments, 12−25 Å in diameter.

The main constituents of the glycocalyx are carbohydrate and protein polymers and copolymers that form a bounded layer around the cell. This polymeric layer is the cell's primary interface with the extracellular aqueous medium and is a thin, true solution colloid. As red blood cells flow around the vascular system they "slip and slide" over vascular surfaces because of the repulsive properties of this polymer layer. Nature, uses this kind of layer to make cell surfaces, first and foremost, mutually repulsive. However, and herein lies a fundamental lesson for biosurface engineers, biosurface selectivity is at the root of mechanisms that control specific ligand−receptor binding and cell−cell recognition. The intersurface repulsion, presented by the, often charged, polymeric surface layer, allows for the operation of selective, chemical attraction when it is combined with specific receptors. This is an area that is currently being explored and will be the basis for the development of designer biomaterials. There are therefore features of this polymer lipid system which should be pertinent to all biomaterials that must interface with biofluids and it therefore represents a prototypical biomaterial, since this kind of highly hydrated polymeric structure is an ideal barrier to oppose biointerfacial and chemical degradation mechanisms of uptake.

As discussed earlier, several researchers have recently shown that the incorporation of glycolipids or a lipid that contains a large polymeric polar headgroup into liposomes does in fact greatly enhance the circulation time of the injected dose of liposomes and their contents in the blood. In order to provide quantitative data with which to evaluate such mechanisms of liposome blood clearance, we have carried out a characterization of interactive and mechanical properties of lipid bilayer systems of typical liposome formulations containing phospholipids, cholesterol, G_{M1}, and a polyethylene glycol lipid (^{2000}PEGDSPE, i.e. distearoyl phospatidylethanolamine with covalently attached methoxy PEG with the degree of polymerization $n \approx 50$) so that we might compare the ability of different types of liposomes to remain in blood circulation vs their mutual interactive and mechanical properties.[66,67]

This X-ray method has proven utility in studies concerning a variety of interbilayer repulsive pressures such as short-range steric, hydration, electrostatic and fluctuation interactions.[88,90,95,113−115,117,121]

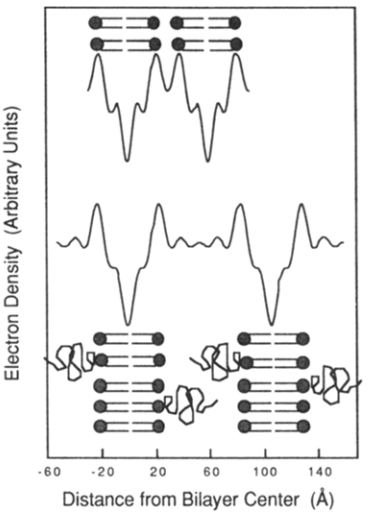

Figure 16. Electron density profiles for 2/1 SOPC/C bilayers in the absence (top profile) and presence (bottom profile) of 4 mol % PEG-lipid. The profiles are at a relatively high applied pressure of 2.8×10^7 dyn/cm^2 (ln $P = 17.2$), giving an interbilayer gap of 51 Å. Two adjacent bilayers are shown in each profile; the origin is located at the center of the left bilayer. For the profile with PEG-lipid, the medium density region, which extends from about 30 to 80 Å corresponds to the interbilayer gap which contains grafted-polymer. (Reprinted from ref 9. Copyright 1964 Elsevier Science Publishing Co., Inc.)

By using this X-ray technique, information has been obtained regarding the extension distance of polymer away from the lipid surface and the magnitude and decay characteristics of the repulsive pressures that exist between surface polymers. An important feature of the approach is that mutual repulsive pressures are measured in a free-standing multilamellar liposome preparation that is sufficiently similar to the liposome drug delivery system to make comparisons meaningful. Multilamellar suspensions were examined with and without 4 mol % PEG-lipid in stearoyloleoylphosphatidylcholine/cholesterol (SOPC/C, 2/1) bilayers. Data was also included for 10 mol % GM1 since this ganglioside has also been shown to prolong liposome circulation half-lives in vivo.[23,67,122]

X-ray data was obtained from these multilamellar suspensions in 100 mM NaCl while applying osmotic pressures and from oriented multilayers in a humid atmosphere. Figure 16 shows electron-density profiles of lipid bilayers made from SOPC/C, 2/1 mixtures in the presence and absence of 4 mol % PEG-lipid at the same applied osmotic pressure.[65] These electron-density profiles give important structural and property information; they confirm that the lipid is well mixed and that it is in the liquid crystalline phase and not the gel phase; they show where the edge of the bilayer is; they demonstrate that the polymer is present in the interbilayer gap; and they give accurate measures of bilayer thickness and interbilayer gap separation in response to applied pressure. Thus, at these low concentrations the addition of PEG-lipid increases the distance between adjacent bilayers, but does not modify the basic bilayer structure.

Figure 17 show plots of the natural logarithm of applied pressure (ln P) vs distance between adjacent

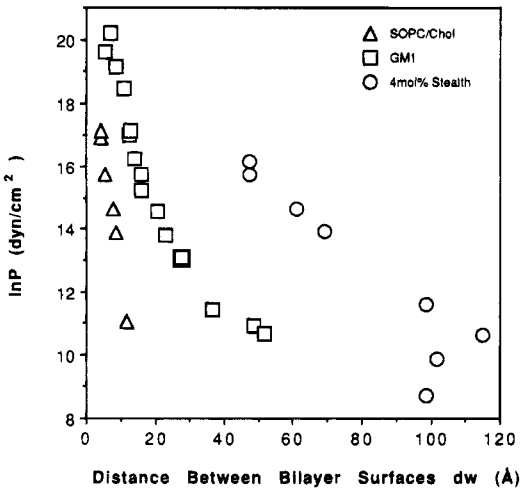

Figure 17. Pressure vs distance between bilayer surfaces for bilayers composed of 2/1 SOPC/C, (△) egg PC/GM1 10 mol % (□); SOPC/PEG-lipid 4 mol % (○). To obtain pressure vs fluid space relationships, osmotic pressures in the range of 0 to 6 × 10^7 dyn/cm^2 were applied to lipid multilayers and the distance between bilayers at each applied pressure was obtained from electron density profiles.

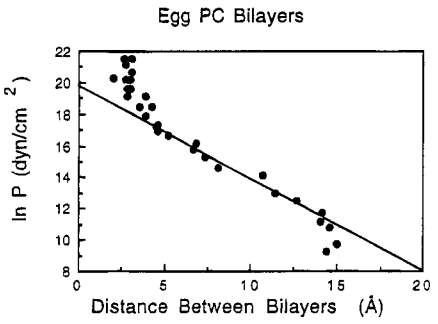

Figure 18. Plot of logarithm of applied pressure vs interbilayer separation distance for egg PC bilayers. The exponential decay is widely believed to be due to water of hydration. At extremely high applied pressures of tens of atmospheres and close separation (~3 Å) a sharp break in the relation indicates a steric repulsion due to headgroup–headgroup interaction.

bilayers for the three systems studied: SOPC/C; SOPC/C with 4 mol % PEG^{2000}-lipid; egg phosphatidylcholine (EPC) with 10 mol % G_{M1}.[67] It is clear that the incorporation of PEG-lipid increases bilayer separation compared to the unmodified lipid surface, for all values of applied pressure. At the smallest applied pressure (ln P = 8.7), the interbilayer gap between PEG-lipid bilayers was ~100 Å compared to only 15 Å for unmodified SOPC bilayers. An indication of the distance that the polymer extends from the lipid surface can be obtained from this onset of the repulsive pressure if we assume that the two polymer-grafted layers interact at their extremum of equilibrium extension. Then, an interbilayer gap of 100 Å implies that the polymer chains extend about 50 Å from the lipid surface. For comparison, and to illustrate hydration or short-range repulsion, the repulsive force between lecithin bilayers is shown in Figure 18.

For the bilayers containing 10 mol % G_{M1}, the tail of the repulsion can be modeled by an electrostatic interaction and so we see that GM1 provides only a weak steric barrier, in line with conclusions from other studies of ganglioside barrier activity.[23]

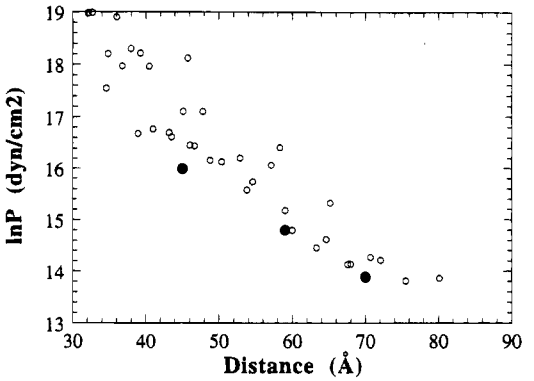

Figure 19. Repulsive pressure (P) between supported DSPE bilayers containing 4.5 mol % ^{2000}PEG-DSPE as calculated from the surface force apparatus measurements which yield force between curved surfaces (F/R) (ref 53) via $F/R = 2\pi E(D) = 2\pi \int P(D)\, dD$ and where E is the energy between flat planes at distance D (○). Solid symbols show data from Figure 17 as measured by osmotic stress technique. Very good agreement between the techniques can be observed. (Courtesy of Tonya Kuhl, UCSB.)

This X-ray data, then, implies (i) the polymer chains extend at least 50 Å from the bilayer surface and (ii) close approach between bilayers is opposed by a long-range repulsive pressure. Thus, the initial interaction of macromolecules (such as plasma proteins) and cellular surfaces with these PEG-grafted bilayers is probably limited to a distance of ~50 Å from the Stealth liposome surface, and any closer approach is met with a significant resistance. Also, when receptor moieties are incorporated in the Stealth liposome surface[27,123,124] these data allow receptor size, especially its spacer arm length, to be matched with polymer extension length. Recently, as mentioned before, chemistry has been developed to allow linkage of antibodies to the far end of the polymer chain.[31,125–127]

Equilibrium force profiles between bilayers doped with various amounts of PEG-lipids have been measured also by the surface force apparatus.[70] Three ^{2000}PEG-lipid concentrations within DOPE (dioleoyl phosphatidylethanolamine) bilayers were studied: 1.3, 4.5, and 9 mol %. Measurements have shown asymptotically decaying tail as opposed to the steep profile predicted by the Alexander–de Gennes theory. After subtracting the long-range electrostatic contribution the agreement between theory and experiment is very good. The influence of temperature was also studied. Theoretically, the elevated temperatures should increase stretching of the chains due to increased osmotic force while at the same time higher temperatures should increase thermal fluctuations and chain contraction due to the fact that water is becoming a poorer solvent. It seems that the effects cancel out because, experimentally, only a very small change in polymer thickness was observed.[53] At packing densities of 43 Å^2 per molecule, the polymer layer thickness of 35, 40, and 70 Å above the bilayer were determined for 1.3, 4.5, and 9 mol % of ^{2000}PEG-DSPE, respectively, in close agreement with X-ray data (Figure 19).

Conformational changes in monolayers of PEG-lipids and their mixtures with phospholipids were measured by film balance experiments and fluorescent microscopy. Two phase transitions were ob-

served: at low coverages pancake–mushroom and at higher mushroom–brush. In the pancake state phase segregation was observed. Only when a depletion layer was formed in the mushroom regime the lipid molecules could intermix with PEG-lipids.[71] Composite polymer-lipid films were deposited on solid substrates and studied by ellipsometry. Disjoining pressures as a function of humidity were studied and it was found that distance vs pressure curves are governed by steric and electrostatic forces and were in good agreement with surface force apparatus and osmotic stress technique measurements.[71] Similar observations were reported also for monolayers with and without PEG-lipids and PEG polymer in a subphase. Free PEG was found to be surface active but could be squeezed from the air–water surface above surface pressures about 10 mM/m.[128–130]

Increasing the concentration of PEG-lipids in the bilayers shows saturation behavior.[33] Bilayer separation increases with PEG-lipid fraction and reaches ca. 170 Å for ^{5000}PEG-DSPE at 6–7 mol %, 115 Å for ^{2000}PEG-DSPE at 7–8 mol % and 60 Å for ^{750}PEG-DSPE at 10–11 mol %, all at applied pressure of 1 atm. This result, as well as in vivo measurements, shows that excess of PEG-lipid, which cannot be incorporated into bilayer due to a high lateral pressure between the polymer coils, probably coexist in the solution in the form of (mixed) micelles. Further addition of the PEG-lipid, which can form micelles in aqueous solutions, results in the dissolution of bilayers into mixed micelles.[32,33,68,69] Small-angle neutron scattering[51] studies of the micelles and cryoelectron microscopy,[157] as well as light scattering[10,25,158] have shown that PEG-lipid micelles are rather small and spherical. Negative stain electron micrograph of transparent solution of lecithin liposomes dissolved with ^{2000}PEG-DSPE show the appearance of long flexible rodlike micelles (data not shown).

Recently, detailed phase behavior of PEG-lipid systems was described in the mixtures of DSPC and PEG-lipids in excess water. Four different polymers, with molecular weights 350, 750, 2000, and 5000 were used. Optical microscopy, turbidity, small- and wide-angle X-ray diffraction, NMR, and differential scanning calorimetry techniques were employed[68] to construct phase diagrams. DSC revealed no polymer phase transitions. The enthalpy of the main transition gel–liquid crystal of DSPC (54 °C) decreases with an increasing amount of PEG-lipid and the transition disappears for the mixed micellar solutions at higher PEG-lipid concentrations. At around 10–20 mol % of longer PEG chains the transition widens and shifts to higher temperatures. Turbidity, X-ray scattering, and NMR measurements have shown that all the systems contain $L_{\beta'}$ (rigid chains, tilted) phase at low PEG-lipid fractions and form micellar phase, M, at higher. In the intermediate regime, however, two different phases are possible: PEG 350 and 750 lipids induce interdigitated phase ($L_{\beta I}$, rigid chains, not tilted, interdigitated) while PEG 2000 and 5000 are in L_β phase (rigid chains, not tilted). At higher temperatures, above transition temperatures, fluid phase L_α (fluid chains, no tilt) are stable while for PEG-lipid contents above 70 mol % (^{750}PEG-lipid), 55% (^{2000}PEG-lipid) and 80% (^{5000}PEG-lipid) micellar phase M (isotropic mixed micelles, nonviscous, nonbirefringent) is stable. Micellar phase is stable also below T_c. ^{350}PEG-lipid, due to very small polar heads, does not form micellar phase and is at high PEG-lipid fractions either in $L_{\beta I}$ phase (below 54 °C) or in L_α phase.[68]

5. Theoretical Studies

5.1. Polymer Extension and Interbilayer Repulsion

In order to characterize the actual surface structures that promote steric stability in the kinds of polymer-grafted lipid bilayer systems that are used to give the Stealth effect, theory and experiment are required that measure both the extension length of the polymer away from the bilayer surface and the repulsive pressures that the grafted polymers exert upon compression. Two types of theories have been developed for systems in which polymers are adsorbed, grafted, or depleted at surfaces:

(i) Scaling theory gives a qualitative description of the polymer surface systems and addresses the physical basis for polymer adsorption,[131–133] depletion,[131–134] and the grafted state.[134–136]

(ii) Mean field theory considers how the polymer chains "feel" a self-consistent mean field due to the chains themselves.[137,138] Cases have been considered where the polymer is adjacent to a surface to which it adsorbs[131] or does not adsorb.[140,141] Milner et al. have studied the behavior of densely-grafted polymers in terms of the mean field approach and describe the case for a stretched surface brush.[142–145]

As discussed earlier, the preliminary results obtained from X-ray diffraction of PEG polymer at the surface of a lipid bilayer were for the low grafting density regime (4 mol % PEG-lipid in PC/cholesterol bilayers). Mean field theories are mostly applicable to more dense systems in the semidilute regime and so the first interpretation of these results has been based on the de Gennes scaling laws for athermal solvents.[65,133,146,147] In this theoretical treatment, we have extended the semiquantitative scaling theories for low grafting concentrations and obtained quantitative results in order to represent the compression of the surface polymer.

Strictly speaking, these theories are for random coils and for the purpose of this theoretical treatment it was supposed that although the grafted PEG chain may have some local helical order, overall it behaves quite randomly as a distorted helix.[148–152] It is also expected that the whole PEG-lipid molecule exhibits rotational diffusion and rotates around its normal axis in the lipid bilayer. Averaging over time, the PEG chain is therefore expected to sweep out a volume that is approximately equivalent to a random coil in an athermal solvent.

5.2. Equilibrium Polymer Chain Extension L for a Single Bilayer Surface

In the deGennes scaling scheme 4 mol % of ^{2000} PEG-lipid in the lipid cholesterol bilayer corresponds to the "mushroom" regime;[135] i.e., the lateral distance

between grafting points is greater than the average size (end-to-end distance) of the PEG random coil and there is no lateral overlapping of polymer chains. When the system is in equilibrium and the free energy of each chain is at a minimum, the chains form separate coils that extend to a distance L from the surface of the bilayer. The polymer extension distance is important because it will determine at what interbilayer gap separation the two polymer surfaces will come into contact and start to interact.

The fact that PEG is a nonadsorbing polymer[141,149] has been taken into account in order to calculate L. The local concentration near the surface is expected to be less than in the PEG random coil giving rise to a polymer depletion layer. Thus, for the equilibrium extension of the nonadsorbing but grafted polymer, we obtain $L = 7/5R_F$, where $R_F = 33.5$ Å. (R_F is the Flory radius and represents the end to end distance of the random coil.) This gives $L = 47$ Å in excellent agreement with the experimental value of 50 Å from X-ray measurements.

5.3. Interbilayer Repulsive Pressures, P_{conf}, between Adjacent Surfaces

If, in the mushroom regime, the PEG polymer chain is compressed from its equilibrium extension it will respond with a conformational elastic pressure P_{conf}, resembling that of a compressed spring. In our lipid bilayer X-ray experiments, this compression is brought about by the forced apposition of a similar polymer surface. In contrast, in the Stealth action of the polymer in the blood stream we would imagine that the other surface is a protein molecule or phagocytic cell membrane. For small compressions this is the only force that opposes the externally applied pressure because the chains are dilute and there is no lateral interaction between them. An excluded volume term only comes in when the chains are sufficiently compressed that they overlap laterally.

Our theoretical analysis[85] is based on general scaling arguments for the conformational energy of a coil trapped in a tube[133] and incorporates numerical coefficients into the scaling theory to provide an equation that is the same as de Gennes except for the coefficient $^5/_2$:

$$P_{conf} = (^5/_2)(kTN)/(D^2a)(a/(d_w/2))^{8/3}$$

where $N = 43$ is the degree of polymerization, $a = 3.5$ Å is the monomer size, $D = 35.7$ Å is the distance between grafting points, and d_w is the separation distance between bilayers. The equation is for d_w less than $2L$. As shown in Figure 20, this prediction (involving no free parameters) is in good agreement with the magnitude of the measured repulsive pressure measured in the range 50 Å < d_w < 100 Å.[66] A similar polymer extension was also estimated from electrophoretic studies.[153] Comparable extensions were also found also for hydrophilic-hydrophobic diblock polymers (polyvinyl pyridine–polystyrene and polyvinyl pyridine–polyisoprene)[154] and the data could be described by a self-consistent mean field theory.[155] Similar dimensions of polymers were found also in PEG-lipid microemulsions.[156]

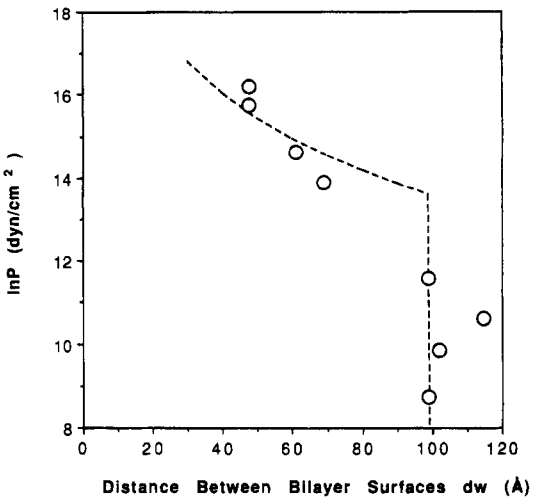

Figure 20. Theoretical interpretation of the experimental data for PEG-lipid bilayers. The theory, shown as a solid line, is derived from scaling laws that describe the interbilayer pressure due to elastic compression of the surface polymer. Experimental data is shown for SOPC/C/PEG-lipid 4 mol % (○).

For d_w around 100 Å the experimentally measured repulsive pressure shows a precipitous drop, as does the predicted value which must necessarily fall to zero at $2L$. Thus, the conformational elastic compression of the polymer chains as "mushrooms" appears to be a good representation of the steric effect for this particular ^{2000}PEG polymer at the lipid bilayer surface at 4 mol %.

Surface force apparatus results, which are in general in a very good agreement with the X-ray determined force–distance profiles (Figure 19), could be also fitted by the two models.

At low coverages (dilute mushroom) Dolan and Edwards' mean-field theory of steric forces and scaling model described experimental data satisfactorily while at higher coverages Alexander–de Gennes theory based on scaling concepts described the data better[70] and a more complex MWC mean field treatment did not bring any better fit.[34] At low coverages, in the mushroom regime the Dolan and Edwards' expression for force between two curved cylindrical surfaces of radius R can be described by

$$F_c(h)/R = 72(kT/D^2)\exp(-h/R_g)$$

where R_g is the radius of gyration of the polymer in a θ solvent and corresponds to the thickness of extending polymer and can be in good solvents substituted by R_F. Despite an underestimation of the polymer layer thickness in the low coverage regime both models are able to fit the force–distance profiles rather well.[70] Scaling analysis fit, which also describes the measured dependence rather satisfactory, can be expressed as

$$F_c(h)/R = 1.6(2kT/D^2)[(R_F/h)^{5/3} - 1]$$

where the numerical prefactor is close to expected unity.[34,70]

At higher grafting densities, i.e. in the brush regime, the force could be described by

$$F_c(h)/R = (16kT\pi h_c)/(35D^3) \times [7(2h_c/h)^{5/4} + 5(h/2h_c)^{7/4} - 12]$$

where

$$h_c = D(R_F/D)^{5/3}$$

Force between two cylindrical surfaces (F_c) and repulsive pressure (P) can be calculated using Derjaguin approximation

$$F_c(h)/R = 2\pi \int P(h)\, dh$$

The agreement with theory was good up to the distance of two polymer layers. At larger separations, the theory, however, predicts steep decrease which was not observed. Obviously, by simply taking into account polydispersity of polymer as well as polymer configurations would alleviate this inconsistency, as will be shown below. Good agreement with this simple scaling concept was observed also in the regime of interacting mushrooms.[68,69]

The above-described experiments and theoretical studies provide a valuable insight to the liposome engineer in order to improve the performance and biological stability and therefore performance of liposomes. Increasing PEG-lipid concentration above a certain fraction will cause bilayer destabilization into mixed micelles. Another critical concentration is the saturation concentration of PEG polymers above the bilayer. This occurs in the brush regime, and the lateral pressure affects mechanic properties of the bilayer. For instance, it reduces tensile strength of the bilayer and therefore liposome stability is a compromise between mechanical stability of the bilayer, which starts to decrease above mushroom–brush transition and colloidal stability.

Force–distance profiles from ref 68 were fitted by current models. Even better agreement was observed when at low PEG-lipid densities (below 1%), a regime of interdigitated mushrooms was introduced and polymer polydispersity was taken into account.[69]

How might these models be applied to biological situations? At present it is still not clear which conformation, i.e., mushroom or brush, is more effective in the prolongation of circulation of liposomes in the blood stream. As equations show, the brush conformation is more effective for the stabilization in vitro. According to the experimental results, optimal steric repulsion is achieved when the bilayer is saturated with polymer-bearing lipid. At higher concentrations these molecules simply form a different and separate phase.[32,33] Theoretical analysis, as shown by Kuhl et al.,[34] also shows that electrostatic repulsion decreases with increasing grafting density.[69] This would also improve stability of liposomes in media with low ionic strength due to reduced effective surface charge, i.e. charge at the slip plane–ζ potential.

In vivo results show, accordingly, that longer circulation times are observed at nonsaturable PEG-lipid fractions, i.e., at concentrations around the mushroom–brush transition.[29,157,158] Above we have discussed mechanistic origin of reduced surface adhesivity. Biological systems, however, may contain also some time-dependent component. While in the above theories it is assumed that polymer is in a good solvent and therefore flexible, protein adsorption may also depend on the contact times which may depend in turn on the flexibility of the chains[25,159–162] and rate of protein conformational changes. It is possible that the optimal stability in blood is a balance between steric repulsion, which increases with the surface coverage, and flexibility of the chains, which decreases with grafting density and size of the polymers and which might be important to reduce protein adsorption.[122,159–162] Comparisons with latex particles containing adsorbed block copolymers PEG-PPO (polypropylene oxide), which also show maximal blood circulation times around mushroom–brush transition, and which show shorter blood circulation times at similar sizes, may indicate that at similar polymer length the more mobile, on one end attached PEG, renders better repulsion and higher flexibility.[162] In addition to measurements of steric repulsion, NMR (and EPR) relaxation measurements of the PEG chain, especially the terminal methyl, should be performed to help interpret these results.

6. Applications and Future Prospects

6.1. Medical Applications of Stealth Liposomes

Due to their ability to evade quick clearance by the immune system, stealth liposomes provide an entirely new and unique drug delivery vehicle. Only by using such liposomes, the goal of Ehrlich's magic bullet, (i.e. a drug delivery system which would target only the diseased cells) has became more possible. Indeed, early studies of Stealth immunoliposomes have shown increased delivery of antibody labeled Stealth liposomes to the target tissue.[124] Still remaining is the problem of delivering the encapsulated drug into the target cell cytoplasm. This problem arises because the majority of cells are not phagocytic and fusion of liposomes and cells is a very rare phenomenon. One approach to overcome this difficulty is to promote liposome–cell membrane fusion by surface attached fusogenic proteins. A simpler way is to try to induce leakage of drug from liposomes in the vicinity of the cell by changes in temperature or pH, or to prepare liposomes with compromised stability. Such liposomes could contain a certain low mole % of monoalkyl surfactants, which upon incubation in the (inter)cellular medium leave the membrane and destabilize liposomes. Alternatively, fast hydrolysis or oxidation of liposomes that have a built-in nonlinear stability profile can also result in liposome destabilization. While this stability issue is one of the current issues in the liposome research, several applications seem still to be effective despite the apparent lack of the drug bioavailability. As will be shown below, these include the delivery of anticancer drugs (anthracyclines) which have shown enormous improvements in therapeutic efficacy upon encapsulation into Stealth liposomes.[10,27]

While antibody-bearing immuno (stealth) liposomes are being extensively studied,[27] currently the

Table 4. Doxorubicin Concentration in Tumor (Kaposi Sarcoma Lesions) of AIDS Patients[a]

dose level (mg/m^2)	DOX (μg/g of tissue)		ratio
	free dox	stealth dox	stealth/free
10	0.18	2.06	11.4
20	0.31	1.61	5.2
40	0.72	7.11	9.9

[a] Data as measured 72 h postinjection of free drug and the same concentration of doxorubicin encapsulated in Stealth liposomes (from ref 185). Data are averages from three patients (two at the highest drug concentration).

most effective way of targeted drug delivery is by passive targeting via extravasation of long-circulating liposomes at or near the sites of increased vascular permeability.[10,163,164] These sites are normally in tumors and at sites of inflammations and infections and are due to the fact that the body has to increase influx and efflux from these sites in order to repair the harm as well as due to physical damage.

According to current understanding[163] the prolonged presence of liposomes in blood allows them to extravasate into sites where the vasculature is leaky such as in tumors.[164-167] Indeed, experiments in animals and humans have shown a 10-fold increase in drug concentration in tumors as compared to free drug (Table 4). In these cases, it seems that liposomes leave the vasculature and are trapped in the tissue where they slowly release their contents either by nonspecific leakage or due to the bilayer degradation by enzymes, such as phospholipases. This coincides with the observation that peak drug levels in tumors are observed 3–4 days after liposome administration as compared to few minutes to hours for the free drug.[168,169] At the peak level, however, the concentration of the drug can be 10–30 times higher in the case of stealth liposome encapsulated drug.[170] In addition to standard action of doxorubicin (mostly intercalation in the DNA and termination of cell replication), high drug concentrations at these sites can cause necrosis of blood vasculature and cuts the blood supply to the tumor.[67,27]

Because of the altered biodistribution of stealth liposomes, the safety of a particular liposome formulation has to be carefully checked. Conventional liposomes are taken up almost entirely by the cells of RES system, whose function is to cope with toxic substances. Although several studies have shown that empty Stealth liposomes are safe to administer, the unnatural biodistribution means that each formulation containing potentially toxic drug has to be tested for its toxicity and maximal tolerated dose. In some cases, this altered biodistribution (mostly from liver and spleen toward skin), can be used for the delivery of various drugs to these tissues.

Figure 21 shows the effect of various treatments on the tumor size in a C26 solid tumor mice model, which is practically insensitive to treatment with free adriamycin (Doxorubicin hydrochloride) and treatments with conventional liposomes containing the drug.[170] A mixture of empty liposomes with free drug, as well as empty liposomes alone, as controls, did not have any significant efficacy compared to untreated, (i.e. saline-injected) animals. The administration of stealth liposomes containing adriamycin

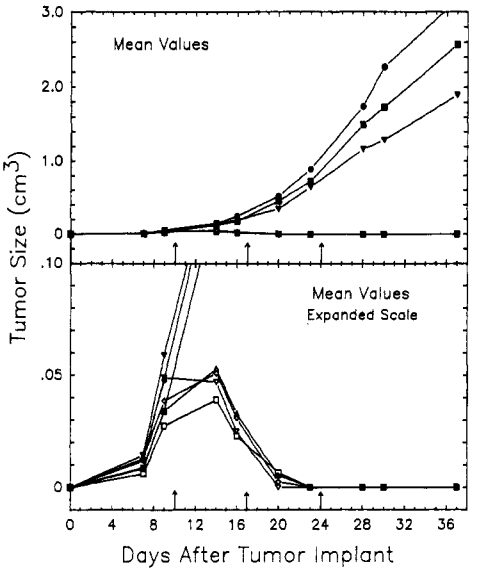

Figure 21. Time dependence of tumor size of solid C26 tumors in mice as a function of different treatments: (●) saline control, (■) free Doxorubicin at 6 mg/kg, (▼) free epirubicin at 6 mg/kg, (□) stealth doxorubicin at 6 and (△) 9 mg/kg. In the expanded scale also stealth epirubicin at 6 (▽) and 9 (◇) mg/kg is shown, respectively. For details see ref 149.

however resulted in complete remission of tumors in the case of early treatment and in significant improvements in animal survival for established tumors. Practically identical results were obtained with the very similar drug epirubicin.[171]

Similar improvements were achieved also in other tumor models, such as mammary carcinoma.[172] In these studies adriamycin in buffer, encapsulated in conventional liposomes (egg phosphatidyl choline EPC, EP glycerol, cholesterol, *dl*-tocopherol = 7/3/4/0.2 mol, 237 nm, encapsulation efficiency EE = 90%) and in stealth liposomes (polyethylene 2000 distearoyl phospatidylethanolamine, hydrogenated soy PC, cholesterol, *dl*-α-tocopherol = 5.5/56.1/38.2/0.2 mol) were tested in the treatment of recently implanted and well-established growing mouse mammary carcinoma and inhibition of the development of spontaneous metastases from intramammary tumor implants. It was found that Stealth liposome encapsulated drug was significantly more effective than either free drug or the drug in conventional liposomes (Figure 22). Several improvements were observed for Stealth liposomes over these two formulations, which themselves did not differ much from the placebo: (i) the incidence of metastases from intramammary implants of tumors (MC19 and MC65) was reduced; (ii) mice with recent implants of tumors MC2A, MC2B, and MC65 were cured; and (iii) the 8-week survival of mice with well-established implants of tumor MC2B was increased. Figure 22 shows the treatment regime at days 3, 10, and 17 as well as at days 10, 17, and 24 after implantation for the tumors MC2A and MC2B. The Stealth formulation is more efficient in the MC2B model because it is slow growing tumor, with in vivo doubling time of 15 days as compared to 4.5 days for the MC2A tumor.

This Stealth formulation also proved to be more effective in the treatment of human lung cancer

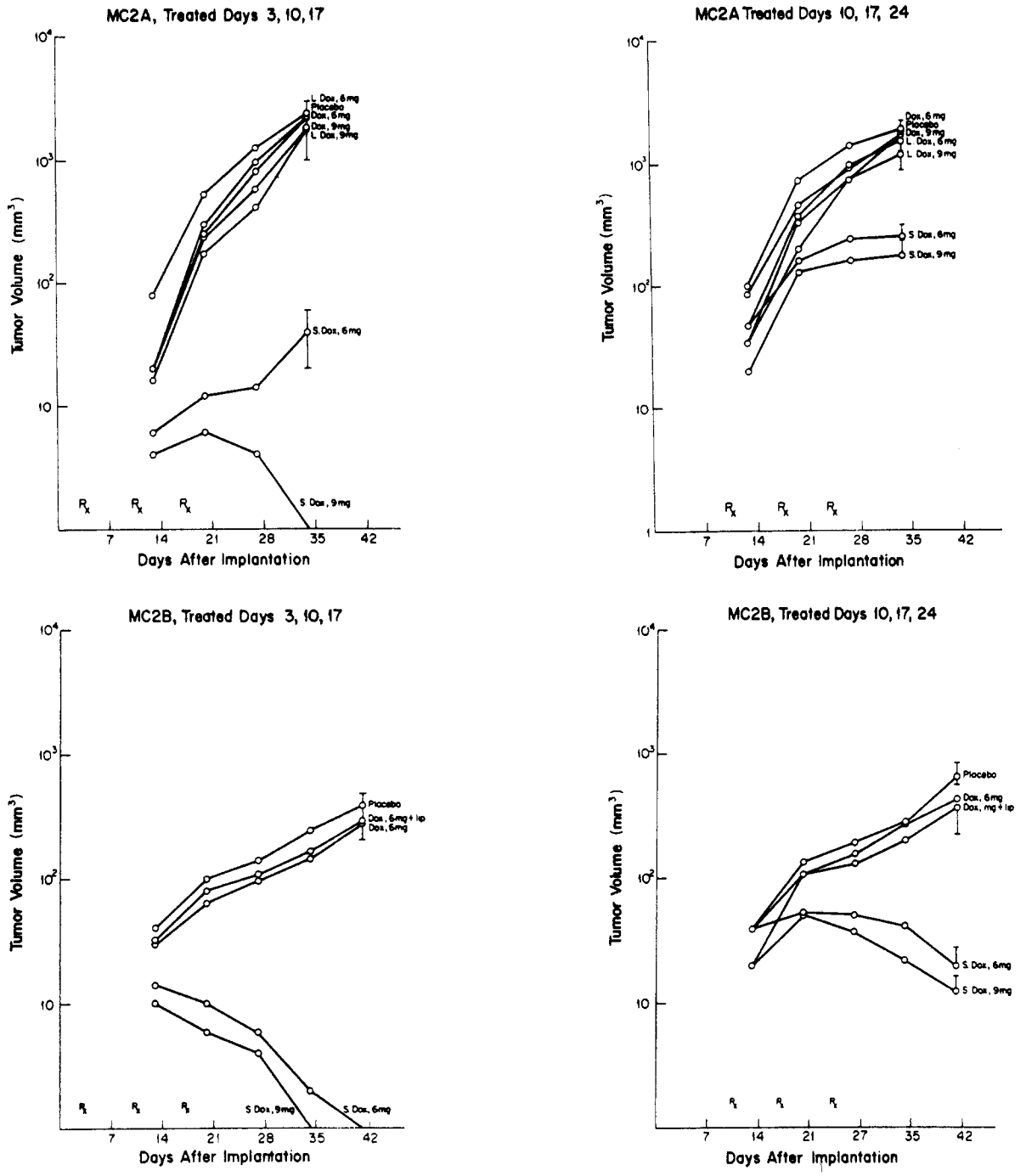

Figure 22. The effect of various treatments on the tumor volume. Two different tumors, a fast growing MC2A (doubling time 4.5 days) and a slow growing MC2B (doubling time 15 days) were selected and treatments, i.e. intravenous injections (in mg/kg) of placebo (buffer), free doxorubicin in buffer (Dox), doxorubicin in conventional liposomes (L-Dox), mixture of Dox and empty Stealth liposomes (Dox + lip.), and doxorubicin in Stealth liposomes (S-Dox), were performed on day 3, 10, and 17 or 10, 17, and 24 after tumor implantation. Adapted from ref 151.

xenographs in scid mice.[173] Free drug and doxorubicin encapsulated in conventional liposomes only slowed down the tumor growth rate from 1.1 cm^3/week to 0.5, while the stealth formulation employing the same drug, arrested the growth at 2 mg/kg and 100% of mice survived to week 12. Treatment also showed a linear dose response what enables better dosing protocols to optimize efficacy and minimize toxicity.[173,174]

The same mechanism of extravasation of drug-loaded liposomes at the sites of leaky vasculature was observed also in the treatment of inflammations, which are also characterized by enhanced vascular permeability.[10,27,164,165,175] The same was also observed in mice with lung infections in which the selectivity ratio of accumulation of Stealth liposomes in the infected lung vs the noninfected one was between 3 and 6.[176]

In addition to passive drug delivery at leaky vasculature sites, there are several other applications which can benefit from the prolonged blood circulation of liposomes and their apparent resistance to macrophage uptake. Long-circulating liposomes with tailored permeability properties can serve as a systemic microreservoir of encapsulated material while localized administration offers a way to deposit drugs

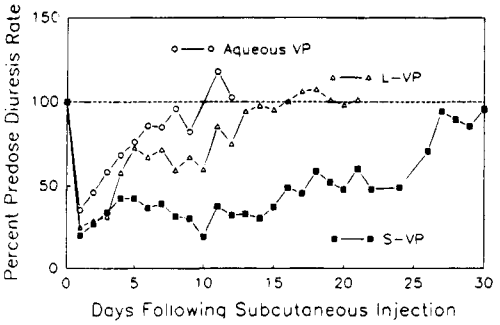

Figure 23. Antidiuretic effect of peptide vasopressin at 50 μg/rat, administered as free drug (○), in conventional liposomes (△), or in Stealth liposomes (■). For details see ref 157.

at subcutaneous and intramuscular sites, or upon inhalation, as intrapulmonary drug depots. An example of a treatment that uses a long circulating microreservoir is studies of stealth liposome encapsulated-cytosine arabinose that have shown improved effect even over 24 h infusion and represent currently the best treatment.[177] Prolonged delivery of encapsulated drugs, such as recombinant peptides and proteins (biopharmaceuticals) can be used also in the nonsystemic applications, such as subcutaneous or intramuscular drug depots. For instance, peptide vasopressin when encapsulated into Stealth liposomes showed activity up to a month while in normal liposomes its activity disappeared within a week[178] as can be seen on Figure 23. Furthermore, fusogenic activity of PEG-coated liposomes at particular coating densities,[179] which can be understood by the phase transition of the polymer (condensation),[148,180] may be of interest for delivery of genes and antisense oligonucleotides. Recent discovery that sterically stabilized liposomes containing a cationic amino group on the far end of PEG chain exhibit, in contrast to normal cationic liposomes, high biological stability[181] may result in novel DNA–liposome complexes for gene therapy.[182,183]

Many new drugs, such as antibiotics, antivirals, and antiinflammatory drugs, are being currently monitored and tested for the encapsulation into sterically stabilized liposomes. Phase I and II clinical trials in humans have yielded very encouraging results. It was found that blood circulation times in humans are around 45 h,[169,174] and at reduced toxicity very good response in AIDS patients with Kaposi sarcoma was observed.[170,184] The high efficacy of the treatment was due not only to the reduced toxicity (leucopenia and neutropenia) of the formulation but also to the approximately 10-fold higher drug concentration that accumulated in tumor lesions (Table 4).[185]

Artificial blood is another possibility where PEG-liposome based hemoglobin carrier system may be beneficial. All current substitutes, including conventional liposomes laden with hemoglobin, severely compromise the immune system and increase the susceptibility of the organism to infection. When PEG-coated liposomes were used significantly reduced immunotoxicity of artificial blood carrier has been demonstrated as measured by host resistance to infectious insult.[186]

Sterically stabilized liposomes composed with mechanically the strongest bilayers are very resistant to the detergent-induced lysis and attack of enzymes. This, coupled with the refractiveness of membranes as introduced in section 4.1, also offers a possibility for orally delivered liposomal dosage forms which can survive the liposomicidal environment in the upper part of the digestive tract. It is known that in several cases improved drug adsorption results when conventional liposomes are applied intragastrically; thus PEGylated liposomes or liposomal hydrogels with tailored physicochemical properties may offer a new development in liposomal applications. The same may also apply to the application of suppositories.

Apart from the above mentioned applications, these systems can be also used as a model system to study various fundamental aspects of colloidal stability, cell biology, and immunology. Due to the novelty of PEG-grafted liposomes, these studies, however, have yet to be performed.

In addition to sterically stabilized liposomes several other Stealth microparticulate systems can be designed: nano and microparticles, (mixed) micelles, and (micro) emulsions. The latter two, however, are probably more interesting in academic research than in practical applications due to inherent instability of these structures upon changes in the environment.

6.2. Biocompatible Surfaces

Up to now, the design of long-circulating liposomes has not been directly compared to the very prolific field of blood biocompatible materials. In these studies many different physicochemical properties of the surfaces which come in contact with body fluids and critically influence their behavior, including blood clotting, were examined. Proteins adsorb avidly to practically all surfaces and many different approaches have been tried to reduce this adsorption. In general, two strategies are being followed to improve the compatibility of the surfaces which come in contact with blood. One uses coatings with antithrombogenic materials, such as heparin, while the other approach tries to minimize protein and cellular adsorption with coatings that include various water-soluble synthetic polymers, such as PEG, and polysaccharides. While heparinized liposomes have not been tried yet, PEGylated liposomes closely resemble the approach of PEGylated surfaces which seems to be the most promising strategy. Many researchers in this field use the phrase polyethylene oxide (PEO), which is synonymous with polyethylene glycol (PEG) and was historically used to describe longer chains.

Among the many polymers studied the best results so far were obtained by PEG-coated surfaces. As we have described, it is speculated that this is due to the (i) low interfacial free energy with water, (ii) unique solution behavior of PEG, (iii) its molecular geometry (thin, high anisotropy), conformation, hydrophilicity, high flexibility and steric stabilization effects. The low interfacial free energy means that there is a low driving force for protein adsorption. Because several other polymers, such as dextran, agarose, methylcellulose, polyacrylamide, and some others, are also characterized by low interfacial tensions but appear to be more interactive, other

mechanisms may be involved to explain the improved passivity of PEG-coated surfaces. PEG polymer avidly forms H bonds with water and between two and three molecules bind to a segment in a tetrahedral conformation. PEG is soluble in water as well as in many organic solvents. Its high solubility in water has been attributed to its structure and ability to form hydrogen bonds and its more random structure in organic solvents. In addition, it is thought, that the rapid movement of hydrated chains influences the microthermodynamics at the interface decreasing the adsorption or adhesion of proteins.[160,187,188] But, undoubtedly, there are other polymers which can impose these properties (see section 2.4). However, its dual solubility in both organic and aqueous solvents may make PEG the most suitable for use as a lipid-grafted agent.

Polymers can be attached to solid surfaces by several different processes including simple adsorption of PEG-containing detergents, block copolymers or high molecular weight polymers, by chemical cross-linking, and by glow discharge which can covalently link the surface adsorbed polymer to the substrate.[188] Studies with polymer-coated surfaces show that the protein adsorption is reduced most effectively in the presence of PEG polymers. Most of the experiments consistently show that lower concentrations of longer chains are better than higher grafting densities of shorter chains, in agreement with measurements of blood circulation times of liposomes containing higher fractions of PEG with molecular weights 350 and 750 Da.[29] Several protein adsorption studies also show that the reduction of adsorption decreases with increasing chain length and it levels off at molecular weights of about 1000 Da.[188,189] This was attributed to the improved hydration, i.e., longer chains have the ability to coil upon themselves and hold more water in weak bonds[189] which exclude high molecular weight solutes from the PEG coils. Another explanation, as discussed earlier, is that adsorption due to van der Waals attraction between particle and surface requires a closeness of approach that is not allowed in the case of longer chains.[10,25]

Briefly, the aggregation is due to ubiquitous van der Waals attraction ($U = -A(b/r)$, A = Hamaker constant, b = particle radius, r = separation.[98,91,190] For optimal steric stabilization of colloidal particles the surface has to be fully covered with an inert, solvent compatible, and flexible polymer. In a good solvent polymer extends $h_c = DN(a/D)^{1/v}$ where N is degree of polymerization, a size of monomer, and D the mean distance between grafting points. In good solvent exponent is $^3/_5$. General criterion for good stabilization becomes then $A(b/h_c) < T$, which yields effective stabilization,[190] and in the case of $A/T = 1/10$ one can estimate, that for effective steric stabilization the surface coating has to be 10% of the particle size.[191]

In addition to devices, such as different patches, needles, and implants, which come in contact with body fluids, these nonfouling, protein repellant, and cell nonadhesive surfaces have many other important applications, including sensors, membranes for separation, filtration, chromatographic supports, contact lenses, immunoassays, and coating of storage vessels for particular proteins.[191-197]

7. Conclusion

In conclusion, polymer-grafted liposomes and their applications show an interplay of various sciences, from theoretical physics, colloid and interface science, organic chemistry, to biology, immunology, pharmacology, medicine, anatomy, and oncology. This is a nice example of how complex and elusive problems can be solved by a multidisciplinary approach. Despite these early successes, room for improvements is indicated by comparing Stealth liposome circulation times with those for red blood cells which, at diameter of the disk of ca. 8 μm can circulate for months. In addition to intensified research and the further development of drug-laden stealth liposome formulations, we anticipate significant basic and technological interest in the following areas: (i) optimization of lipid composition, (ii) studies of phase behavior of lipid/polymer−lipid systems and its influence on the liposome properties, including release of encapsulated molecules and (iii) mechanical properties of liposomes, such as intrinsic bending (in the case of uneven distribution of PEG-lipid in the two monolayers of these bilayers). Preliminary data show that PEG-lipid micelles, when mixed with lecithin MLVs slowly incorporate into the bilayers and that some unilamellar vesicles are formed. It is very probable that these vesicles have uneven distribution of PEG-lipid across the bilayer and therefore they may have nonzero spontaneous curvature that can make them thermodynamically stable[10,197-200] and this can be of experimental as well as theoretical interest.[10] The next task is probably to achieve increased blood circulation times for larger liposome sizes (>200 nm). We believe, that a rational approach based on the reviewed facts should be undertaken. Currently the most important issue for the liposome engineering is probably to decide on the optimal composition, meaning mostly the fraction and molecular weight of the incorporated PEG-lipid, which may not necessarily be the same for in vitro and in vivo stability. Also the question of polymer destabilization of the liposome bilayer has not been fully studied yet. For instance, polymer phase transition, such as condensation of a brush or random coil can destabilize the liposome, disrupt the bilayer, or cause phase segregation within the membrane. In contrast to undesired problems of liposome stability or leakage such a transition can be also useful for liposome engineering. For example, if the polymer phase transition can be induced by a particular interaction, such as binding, presence of particular ions, protons, or (macro) molecules, or cleavage of the polymer, this can be used for the triggered drug release or design of fusogenic liposomes. The influence of charge on the PEG-lipid on liposome properties and the distribution of PEG molecules between the two monolayers will also have to be studied. In parallel, of course, the new approach of specific targeting by attaching ligands, such as antibodies, to the far end of PEG chains have been undertaken.

Polymer-bearing lipids have therefore opened a whole new area and era in the research and applica-

tions of liposomes as well as in biomaterials and related fields.

8. References

(1) Stealth is a trademark of Liposome Technology, Inc., Menlo Park, CA.
(2) Bangham, A. D., Ed. *Liposome Letters*; Academic Press: New York, 1983.
(3) Papahadjopoulos, D., Ed. *Ann. N. Y. Acad. Sci.* **1978**, *308*, 1.
(4) Gregoriadis, G.; Allison, A. C., Eds. *Liposomes in biological systems*; J. Wiley: New York, 1980.
(5) Gregoriadis, G., Ed. *Liposomes as drug carriers: recent trends and progress*; J. Wiley: NewYork, 1988.
(6) Knight, C. G., Ed. *Liposomes: from physical structure to therapeutic applications*; Elsevier: Amsterdam, 1981.
(7) Ostro, M. J., Ed. *Liposomes*; M. Dekker: New York, 1983.
(8) Fidler, I. J., Berestein, G., Eds. *Liposomes in the therapy of infectious diseases and cancer*; A. Liss: New York, 1989.
(9) Bangham, A. D.; Horne, W. J. *Mol. Biol.* **1964**, *8*, 660.
(10) Lasic, D. D. *Liposomes: from Physics to Applications*; Elsevier: Amsterdam, 1993.
(11) New, R. R. C., Ed. *Liposomes: a practical approach*; IRL Press: Oxford, 1990.
(12) Barenholz, Y., Ed. *Chem. Phys. Lipids* **1993**, *64*, 1.
(13) Senior, J. *Crit. Rev. Ther. Drug Carr. Syst.* **1987**, *3*, 123.
(14) Torchilin, V. P.; Berdichevsky, V. R.; Barsukov, A. A.; Smirnov, V. N. *FEBS Lett.* **1980**, *111*, 184.
(15) Surolia, A.; Bachhawat, B. K.; Podder, S. K. *Nature* **1975**, *257*, 802.
(16) Allen, T. M.; Chonn, A. *FEBS Lett.* **1987**, *223*, 42.
(17) Gabizon, A.; Papahadjopoulos, D. *Proc. Natl. Acad. Sci. U.S.A.* **1988**, *85*, 6949.
(18) Abuchowski, A.; VanEs, T.; Palczuk, N. C.; Davis, S. S. *J. Biol. Chem.* **1977**, *11*, 3578.
(19) Illum, L.; Davis, D. D. *Life Sci.* **1987**, *40*, 367.
(20) Woodle, M. C.; Newman, M.; Collins, L.; Redemann, C.; Martin, F. J. In *Proceedings of Symposium on Controlled Release of Bioactive Materials*; Lee, V. H., Ed. *CRS* **1990**, *17*, 77.
(21) Klibanov, A. L.; et al. *FEBS Lett.* **1990**, *268*, 235.
(22) Blume, G.; Cevc, G. *Biochim. Biophys. Acta* **1990**, *1029*, 91.
(23) Senior, J.; Delgado, C.; Fisher, D.; Tilcock, G. *Biochim. Biophys. Acta* **1991**, *1062*, 77.
(24) Allen, T. M.; Hansen, C.; Martin, F.; Redemann, C.; Yau-Young, A. *Biochim. Biophys. Acta* **1991**, *1066*, 29.
(25) Woodle, M. C.; Lasic, D. D. *Biochim. Biophys. Acta* **1992**, *1113*, 171.
(26) Huang, L., Ed. *J. Liposome Res.* **1992**, *2*, 186.
(27) Lasic, D. D., Martin, F., Eds. *Stealth Liposomes*; CRC Press: Boca Raton, 1995.
(28) Allen, T. M. *Adv. Drug Delivery Sys.* **1994**, *13*, 285.
(29) Lasic, D. D. *Angew. Chem., Int. Ed. Engl.* **1994**, *33*, 1685.
(30) Lasic, D. D.; Papahadjopoulos, D. *Science* **1995**, *267*, 1275.
(31) Zalipsky, S. *Bioconjugate Chem.* **1993**, *4*, 296.
(32) Lasic, D. D.; Woodle, M. C.; Martin, F. J.; Valentincic, T. *Period. Biol.* **1991**, *93*, 287.
(33) McIntosh, T. J. et al. In ref 27, Chapter 7, p 63.
(34) Kuhl, T.; et al. In ref 27, Chapter 8, p 73.
(35) Woodle, M. C.; Engbers, C. M.; Zalipsky, S. *Bioconjugate Chem.* **1994**, *5*, 493.
(36) Torchilin, V. P.; et al. *Biochim. Biophys. Acta* **1994**, *1195*, 181.
(37) Kronberg, B.; Dahlman, A.; Carlfors, J.; Karsson, J. *J. Pharm. Sci.* **1990**, *79*, 667.
(38) Virden, J. W.; Berg, J. C. *J. Colloid Interface Sci.* **1992**, *153*, 411.
(39) Klibanov, A. L.; Huang, L. *J. Liposome Res.* **1992**, *2*, 321.
(40) Winterhalter, M.; Klotz, K.-H.; Lasic, D. D. Manuscript to be submitted.
(41) Prime, K. L.; Whitesides, G. M. *Science* **1991**, *252*, 1164.
(42) Desai, N. P.; Hubble, J. A. *J. Biomed. Mater. Res.* **1991**, *25*, 829.
(43) Jeon, S. I.; Lee, H. J.; Andrade, J. D.; deGennes, P. G. *J. Colloid. Interface Sci.* **1991**, *142*, 159.
(44) Lee, J. H.; Kopecek, J.; Andrade, J. D. *J. Biomed. Mater. Res.* **1989**, *23*, 351.
(45) Roerdink, F.; Dijkstra, J.; Hartman, G.; Bolscher, B.; Scherphof, G. *Biochim. Biophys. Acta* **1981**, *667*, 79.
(46) Gregoriadis, G. *New Physiol. Sci.* **1989**, *4*, 146.
(47) Evans, E.; Metcalfe, M. *J. Phys. Chem.* **1987**, *91*, 4219.
(48) Winterhalter, M.; Klotz, K. H.; Lasic, D. D.; Benz, R. *Trends Colloid Interface Sci.* **1995**, in press.
(49) Noppl, D.; Needham, D. *Biophys. J.*, in press.
(50) Lasic, D. D.; et al. *FEBS Lett.* **1992**, *312*, 255.
(51) Auvray, L.; Auroy, P.; Lasic, D. D. Manuscript in preparation.
(52) Stilbs, P.; Lasic, D. D. Unpublished data.
(53) Bonte, A.; Juliano, R. L. *Chem. Phys. Lip.* **1986**, *40*, 359.
(54) Szebeni, J.; et al. *Biochem. Biophys. Res. Commun.* **1994**, *30*, 255.
(55) Szebeni, J.; Lasic, D. D.; Alving, C. R. Unpublished data.
(56) Chonn, A.; Cullis, P. R. *J. Liposome Res.* **1992**, *2*, 397.
(57) Chonn, A.; Semple, S. C.; Cullis, P. R. *J. Biol. Chem.* **1992**, *267*, 18759.
(58) Scherphof, G. L.; Roerdink, F.; Waite, M.; Parks, J. J. *Biochim. Biophys. Acta* **1978**, *542*, 296.
(59) Scherphof, G. L. In *Handb. Exp. Pharmacol.* **1991**, *100*, 285.
(60) Moghimi, S. M.; Patel, H. M. *Biochim. Biophys. Acta* **1989**, *984*, 384.
(61) Lee, K. D.; Hong, K.; Papahadjopoulos, D. *Biochim. Biophys. Acta* **1992**, *1103*, 85.
(62) Azuree, V. *Chim. Oggi* **1992**, *10*, 15.
(63) Silvius, J. R.; Zuckermann, M. J. *Biochemistry* **1993**, *32*, 3153.
(64) Parr, J. P.; Ansell, S.; Choi, L.; Cullis, P. R. *Biochim. Biophys. Acta* **1994**, *1195*, 21.
(65) Scotto, A. W.; Seow, H.; Wos, A. *Biophys. J.* **1995**, *68*, A215.
(66) Needham, D.; McIntosh, T. J.; Lasic, D. D. *Biochim. Biophys. Acta* **1992**, *1180*, 40.
(67) Needham, D.; Hristova, K.; Mcintosh, T. J.; Dewhirst, M.; Wu, N.; Lasic, D. D. *J. Liposome Res.* **1992**, *2*, 411.
(68) Kenworthy, A. K.; Simon, S. A.; McIntosh, T. J. *Biophys. J.* **1995**, *68*, 1903.
(69) Kenworthy, A. K.; Hristova, K.; Needham, D.; McIntosh, T. J. *Biophys. J.* **1995**, *68*, 1921.
(70) Kuhl, T. L.; Leckband, D. E.; Lasic, D. D.; Israelachvili, J. N. *Biophys. J.* **1994**, *66*, 1479.
(71) Baekmark, T.; Ellander, S.; Lasic, D. D.; Sackmann, E. *Langmuir*, in press.
(72) Needham, D.; Nunn, R. S. *Biophys. J.* **1990**, *58*, 997.
(73) Needham, D.; Zhelev, D. *Ann. Biomed. Eng.* **1995**, *23*, 287.
(74) Rutkowski, C. A.; Williams, L. M.; Haines, T. H.; Cummings, H. Z. *Biochemistry* **1991**, *30*, 657.
(75) Evans, E. *Physical Basis of Cell-Cell Adhesion*; Bongrande, P., Ed.; CRC Press: Boca Raton, FL, 1988; p 91.
(76) Kwok, R.; Evans, E. *Biophys. J.* **1981**, *35*, 367.
(77) Needham, D.; Evans, E. *Biochemistry* **1988**, *27*, 8261.
(78) Needham, D.; McIntosh, T. J.; Evans, E. *Biochemistry* **1988**, *27*, 4668.
(79) Evans, E.; Skalak, R. *Mechanics and Thermodynamics of Membranes*; CRC Press: Boca Raton, FL, 1980.
(80) Evans, E.; Rawicz, W. *Phys. Rev. Lett.* **1990**, *64*, 2094.
(81) McIntosh, T. J.; Simon, S. A.; Needham, D.; Huang, C. *FEBS Lett.* **1991**, *284*, 263.
(82) Ipsen, J. H.; Mouritsen, O. G.; Bloom, M. *Biophys. J.* **1990**, *57*, 405.
(83) Ipsen, J. H.; Mouritseen, O. G.; Zuckermann, M. J. *Biophys. J.* **1989**, *56*, 661.
(84) diSalvo, E. A.; et al, *Biophys. J.* **1994**, *66*, 1943.
(85) Hristova, K. Ph.D. Thesis, Duke University, 1993.
(86) Hristova, K.; Needham, D. *J. Colloid Interface Sci.* **1994**, *168*, 302.
(87) McIntosh, T. J.; Magid, A. D.; Simon, S. A. *Biochemistry* **1987**, *26*, 7325.
(88) McIntosh, T. J.; Magid, A. D.; Simon, S. A. *Biochemistry* **1989**, *28*, 17.
(89) McIntosh, T. J.; Magid, A. D.; Simon, S. A. *Biochemistry* **1989**, *28*, 7904.
(90) McIntosh, T. J.; Simon, S. A.; Needham, D.; Huang, C. *Biochemistry* **1992**, *31*, 2020.
(91) Israelachvill, J. N. *Surface and interparticle Forces*; Academic Press, Inc.: New York, 1985.
(92) Israelachvili, J. *Q. Rev. Biophys.* **1974**, *6*, 341.
(93) LeNeveu, D. M.; Rand, P. R.; Parsegian, V. A.; Gingell, D. *Biophys. J.* **1977**, *18*, 209.
(94) McIntosh, T. J.; Simon, S. A. *Biochemistry* **1986**, *25*, 4058.
(95) Parsegian, V. A.; Fuller, N.; Rand, R. P. *Proc. Natl. Acad. Sci. U.S.A.* **1979**, *76*, 2750.
(96) Parsegian, V. A.; Ninham, B. W. *J. Theor. Biol.* **1973**, *38*, 101.
(97) Rand, R. P. *Annu. Rev. Biophys. Bioeng.* **1981**, *10*, 277.
(98) Verwey, E. J.; Overbeek, J. T. G. *Theory of the stability of lyophobic colloids*, Elsevier: Amsterdam, 1948.
(99) Israelachvili, J. N.; Wennerstrom, H. *J. Phys. Chem.* **1992**, *96*, 520.
(100) Evans, E.; Parsegian, V. A. *Proc. Natl. Acad. Sci. U.S.A.* **1986**, *83*, 7132.
(101) Tabor, D.; Winterton, R. H. S. *Proc. R. Soc. Lond. A* **1969**, *312*, 435.
(102) Israelachvili, J. N.; Adams, G. E. *J. Chem Soc. Faraday Trans.* **1978**, *74*, 975.
(103) Marra, J. *Biophys. J.* **1986**, *50*, 815.
(104) Marra, J.; Israelachvili, J. *Biochemistry* **1985**, *24*, 4608.
(105) Evans, E. *Biophys. J.* **1980**, *30*, 265.
(106) Evans, E.; Needham, D. *Faraday Discuss. Chem. Soc.* **1986**, *81*, 267.
(107) Evans, E.; Metcalfe, M. *Biophys. J.* **1984**, *46*, 423.
(108) Evans, E.; Metcalfe, M. *Biophys. J.* **1984**, *45*, 715.
(109) Evans, E.; Needham, D. *Macromolecules* **1988**, *21*, 1822.
(110) Evans, E.; Needham, D. *Molecular Mechanisms of Membrane Fusion*; Okhi, S., Doyle, D., Flanagan, T. D., Hui, S. W., Mayhew, E., Eds.; Plenum Press: New York, 1988; p 83.

(111) Luzzati, V.; Mustachi, M.; Skoulios, A.; Husson, R. *Acta Crystallogr.* **1960**, *13*, 660.
(112) Krzywicki, T.; Tardieu, A.; Luzzati, V. *Mol. Cryst. Liq. Cryst.* **1969**, *8*, 285.
(113) McIntosh, T. J.; Holloway, P. W. *Biochemistry* **1987**, *26*, 1783.
(114) McIntosh, T. J.; Magid, A. D.; Simon, S. A. *Biophys. J.* **1989**, *55*, 897.
(115) McIntosh, T. J.; Magid, A. D.; Simon, S. A. *Biophys. J.* **1990**, *57*, 1187.
(116) Simon, S. A.; McIntosh, T. J. *Proc. Natl. Acad. Sci. U.S.A.* **1989**, *86*, 9263.
(117) Simon, S. A.; McIntosh, T. J.; Magid, A. D.; Needham, D. *Biophys. J.* **1992**.
(118) Sackmann, E., Lipowsky, R., Eds. *Hanbook of Membranes*; Elsevier: Amsterdam, 1995.
(119) Helfrich, W. *Z. Naturforsch.* **1978**, *33a*, 303.
(120) Latta, H.; Johnson, W.; Stanley, T. J. *Ultrastruct. Res.* **1975**, *51*, 354.
(121) McIntosh, T. J.; Magid, A. D.; Simon, S. A. *Biophys. J.* **1990**, *57*, 1187.
(122) Lasic, D. D.; et al. *Biochim. Biophys. Acta* **1991**, *1070*, 187.
(123) Agrawal, A. K.; Allen, T. M. *Biophys. J.* **1992**, *61*, A493.
(124) Mori, A.; Klibanov, A. L.; Torchilin, V. P.; Huang, L. *FEBS Lett.* **1991**, *284*, 263.
(125) Blume, G., et al. *Biochim. Biophys. Acta* **1993**, *1149*, 180.
(126) Zalipsky, S. In ref 27, Chapter 9, p 93.
(127) Zalipsky, S. *Bioconjugate Chem.* **1995**, *6*, 150.
(128) Winterhalter, M.; et al. *Biophys. J.* **1993**, *65*, A173.
(129) Burner, H.; Winterhalter, M.; Benz, R. *J. Colloid Interface Sci.* **1994**, *168*, 183.
(130) Winterhalter, M.; et al. *Biophys. J.* **1995**, *67*, A 302.
(131) deGennes, P. G. *Macromolecules* **1981**, *14*, 1637.
(132) deGennes, P. G. *Macromolecules* **1982**, *15*, 492.
(133) deGennes, P. G. *Scaling Concepts in Polymer Physics*; Cornell Univ. Press: Cornell, 1985.
(134) Alexander, S. *J. Phys.* **1977**, *38*, 983.
(135) deGennes, P. G. *Macromolecules* **1980**, *13*, 1069.
(136) deGennes, P. G. In *Physical Basis of Cell-Cell Adhesion*; Bongrande, P., Ed.; 1988; p 39.
(137) Dolan, A.; Edwards, S. *Proc. R. Soc. Lond. A* **1973**, *337*, 509.
(138) Dolan, A.; Edwards, S. *Proc. R. Soc. Lond. A* **1974**, *343*, 427.
(139) Edwards, S. *Proc. Phys. Soc.* **1965**, *85*, 613.
(140) Edwards, S. *Proc. Phys. Soc.* **1966**, *88*, 265.
(141) Evans, E.; Needham, D. *Macromolecules* **1988**, *21*, 1822.
(142) Milner, S. T. *Europhys. Lett.* **1988**, *7*, 695.
(143) Milner, S. T.; Witten, T. A.; Cates, M. E. *Europhys. Lett.* **1988**, *5*, 413.
(144) Milner, S. T.; Witten, T. A.; Cates, M. E. *Macromolecules* **1988**, *21*, 2610.
(145) Milner, S. T.; Witten, T. A. *Macromolecules* **1989**, *22*, 853.
(146) Hristova, K.; Needham, D. *Liq. Crys.* **1995**, *18*, 423.
(147) Arnold, K.; Herrmann, A.; Gawrisch, K.; Pratsch, L. *Molecular Mechanisms of Membrane Fusion*; Okhi, S., et al., Ed.; Plenum Press: New York, 1987; p 225.
(148) Bailey, F.; Koleske, J. *Poly(ethylene) Oxide*; Academic Press Inc.: New York, 1976.
(149) Devanand, K.; Seiser, J. C. *Nature* **1990**, *343*, 739.
(150) Takahashi, Y.; Tadokoro, H. *Macromolecules* **1973**, *6*, 672.
(151) Yang, R.; Yang, X. R.; Evans, D. F.; Hendrikson, W. A.; Baker, J. *J. Phys. Chem.* **1990**, *94*, 6123.
(152) Hristova, K.; Needham, D. *Macromolecules* **1995**, *28*, 991.
(153) Woodle, M. C.; et al. *Biophys. J.* **1992**, *61*, 902.
(154) Watanabe H.; Tirrell, M. *Macromolecules* **1993**, *26*, 6455.
(155) Dan, N.; Tirrell, M. *Macromolecules* **1992**, *25*, 2890.
(156) Safinya, C., et al. Manuscript in preparation.
(157) Woodle, M. C.; et al. *Biochim. Biophys. Acta* **1992**, *1105*, 193.
(158) Lasic, D. D.; Zalipsky, S. Manuscript in preparation.
(159) Andrade, J. D.; Nagaoka, S.; Cooper, S.; Okano, T.; Kim, S. W. *ASAIO* **1987**, *10*, 75.
(160) Nagaoka, S.; et al. *ASAIO* **1987**, *10*, 76.
(161) Blume, G.; Cevc, G. *Biochim. Biophys. Acta* **1993**, *1146*, 157.
(162) Caldwell, K. Private communication.
(163) Papahadjopoulos, D.; et al. *Proc. Natl. Acad. Sci. U.S.A.* **1991**, *88*, 11460.
(164) Dvorak, H. F.; Nagy, J. A.; Dvorak, J. T.; Dvorak, A. M. *Am. J. Pathol.* **1988**, *133*, 95.
(165) Jain, K. *Metastasis Rev.* **1987**, *6*, 559.
(166) Wu, N. Z.; Da, D.; Rudoll, T. L.; Needham, D.; Dewhirst, M. *Cancer Res.* **1993**, *53*, 3765.
(167) Dewhirst, M.; Needham, D. In ref 27, p 127.
(168) Gabizon, A. *Can. Res.* **1992**, *52*, 891.
(169) Gabizon, A.; et al. *J. Liposome Res.* **1993**, *3*, 517.
(170) Mayhew, E.; Lasic, D. D.; Babbar, S.; Martin, F. J. *Int. J. Cancer* **1992**, *51*, 302.
(171) Huang, K. S.; et al. *Cancer Res.* **1992**, *52*, 6774.
(172) Vaage, J.; Mayhew, E.; Lasic, D. D.; Martin, F. J. *Int. J. Cancer* **1992**, *51*, 942.
(173) Williams, S. S.; et al. *Cancer Res.* **1993**, *53*, 3964.
(174) Working, P.; et al. *J. Liposome Res.* **1994**, *4*, 667.
(175) Williams, B. D.; et al. *Br. J. Med.* **1986**, *293*, 1114.
(176) Bakker-Woudenberg, I. A. J. M.; et al. *J. Infect. Dis.* **1993**, *168*, 164.
(177) Allen, T. M.; Mehra, T.; Hansen, C.; Chin, Y. *Cancer Res.* **1992**, *52*, 2431.
(178) Woodle, M. C.; et al. *Pharm. Res.* **1992**, *9*, 260.
(179) Okamura, Y.; Yamauchi, H.; Yamamoto, J.; Sunamoto, K.; *Proc. Jpn. Acad. Sci. Ser. B* **1993**, *69*, 45.
(180) deGennes, P. G. *C.R. Seances Acad. Sci.* **1991**, *313*, 1117.
(181) Zalipsky, S.; Brandeis, E.; Newman, M.; Woodle, M. C. *FEBS Lett.* **1994**, *353*, 71.
(182) Felgner, P. *Adv. Drug. Del. Syst.* **1990**, *5*, 163.
(183) Lasic, D. D. *Chim.Oggi/Chemistry today* **1995**, in press.
(184) Boggner, J.; Goebel, F. D. In ref 27, p 267.
(185) Northfelt, D., et al. In ref 27, p 257.
(186) Zheng, S.; Beissinger, R.; Sherwood, R. L.; McCormick, D.; Lasic, D. D. *J. Liposome Res.* **1993**, *3*, 575.
(187) Lee, J. H.; Kopecek, J.; Andrade, J. D. *J. Biomed. Mater. Res.* **1989**, *23*, 351.
(188) Harris, M. *Poly(ethylene) Glycol Chemistry*; Plenum Press: New York, 1992.
(189) Gombotz, W. R.; Wang, G.; Horbett, T. A.; Hoffman, A. S. In ref 188, p 247.
(190) Pincus, P. A. In *Lectures on thermodynamics and statistical mechanics*, Gonzalez, A. E., Varea, C., Eds.; World Publishing: Singapore, 1988; p 1.
(191) Pincus, P. Private communication 1995.
(192) Gombotz, W. R.; Wang, G.; Horbett, T. A.; Hoffman, A. S. *J. Biomed. Mater. Res.* **1991**, *25*, 1547.
(193) Antonsen, K. P.; Hoffman, A. S. In ref 188, p 15.
(194) Llanos, G. R.; Sefton, M. V. *Biomaterials* **1992**, *13*, 421.
(195) Desai, N. P.; Hossainy, S.; Hubbel, J. A. *Biomaterials* **1992**, *13*, 417.
(196) Kishida, A. *Biomaterials* **1992**, *13*, 113.
(197) Helfrich, W. *Z. Naturforsch.* **1973**, *28c*, 693.
(198) Lasic, D. D. *J. Colloid Interface Sci.* **1990**, *140*, 302.
(199) Kaler, E. W.; et al. *Science* **1989**, *245*, 1371.
(200) Lasic, D. D. *Nature* **1992**, *355*, 279.

CR920044T